

Is a more physical representation of aerosol activation needed for simulations of fog? - Author's response

Responding authors: Craig Poku et al.

March 18, 2021

We would like to thank both reviewers for the detailed and constructive feedback. We have found it beneficial to receive these reviews, as it's allowed us to address weaknesses in the original manuscript and provide new focus on our key scientific outcomes.

1 Reviewer 1's comments and responses

1. line 13-14: the sentence reads odd. The minimum updraft velocity threshold overpredicts the droplet number in comparison to a cooling rate? What you are saying is that a cooling rate underpredicts a droplet number. How can a cooling rate/threshold predict something?

Thank you for this suggestion. We have reworded this line in our abstract to say the following: "Our offline model results show that using the equivalent cooling rate associated with the minimum updraft velocity threshold assumption can overpredict the droplet number by up to 70% in comparison to a typical cooling rate found in fog formation." This can be located on line 13 in our manuscript.

2. Introduction: You elaborate the current state of fog simulation in which often a bulk microphysics scheme is used, nowadays often with aerosol activation parameterization. However, you have missed important recent work that avoids aerosol activation parameterizations by using a Lagrangian cloud model (see Schwenkel and Maronga (2020), <https://www.mdpi.com/2073-4433/11/5/466>). I do think it would be worth to discuss their paper in the introduction. How do your results relate to their LES? Would a direct comparison of the same case make sense? The same authors also recently published a related article in ACP (<https://acp.copernicus.org/articles/19/7165/2019/acp19-7165-2019.html>). You do cite this close to the end of the manuscript, but I would say their work is so closely related to what you did that I would expect that you put your work into context of the two papers in the introduction.

Thank you for making us aware of these papers. Based on your comments, we have expanded our introduction to include more recent literature, including Schwenkel and Maronga (2020), that focuses

on avoiding aerosol activation schemes when investigating fog using LES. We have also discussed the eqs. used in Schwenkel and Maronga (2019) and demonstrated how they can relate to our work. These additions can be found from lines 73-79 and lines 95-97.

3. Eq 6: What is the variable "L"? I think you do not define it at all.

We have defined L as the specific latent heat of vaporisation in Eq. 6 of the revised manuscript.

4. Table 2 / case definition. To be honest, i had serious difficulties to follow your text at some places because the case definition appears a little chaotic. The is best seen in Table 2. Example: Case C_adiabatic has two tests, but for T_ship_ad has all aerosol modes and all environments. So how many simulations were performed? It is very difficult to read the table that way. It would be beneficial to list all simulations in a more straight forward order.

Thank you for this comment. When we went through the manuscript, we could see how the original table appeared confusing. As a result, we have rewritten this table and split it into Table's 2 and 3. These tables now state that for the offline box model runs, we did in total 24 unique tests.

5. In the legend of Figure 1 you refer to "Aitken, accumulation, and coarse model aerosols". However, if you are not an expert in aerosol physics you might not know what these modes are. And this is the first time these terms appear in the manuscript! Please provide an explanation to the reader at a suitable location. It might help to give a schematic diagram showing these modes.

Thank you for this comment. We have added a section about aerosol modes in the introduction to include the following: "The aerosol population is split by size categories. These size categories (hereafter known as modes) are technically defined as: the Aitken mode, where the diameter, d , of an aerosol particle is $< 0.1 \mu\text{m}$; the accumulation mode, where $0.1 \leq d \leq 1.0 \mu\text{m}$; and the coarse mode, where $d > 1.0 \mu\text{m}$ (Whitby, 1978). Due to their size, Aitken mode aerosols have an increased tendency to coagulate with other particles and not activate in their own right. In contrast, accumulation and coarse mode aerosols can activate into fog droplets, therefore indirectly impacting the cloud's microphysical structure and its life span (e.g. Twomey, 1974; Albrecht, 1989)." These sentences can be located from lines 35-40.

6. line 224: How can you motivate a grid spacing without given the grid spacing? Furthermore, you cite studies that clearly state that 1 m grid spacings is best choice, but you use only 2 m. Given the very limited horizontal domain, I have to ask: why did you use such "coarse" grid spacing? It does not make sense to me.

Thank you for pointing this out. Having revised the manuscript, we're aware that this statement (as it was mentioned in our previous study) is quite vague. Therefore, we conducted some tests that focused on changing the horizontal resolution by 1 m (high res) and 4 m (low res). When using a w_{min} of 0.1 m s^{-1} , we found that there was no appreciable difference between the choice in horizontal resolution. However, the choice in horizontal resolution becomes important when w_{min} is lowered to 0.01 m s^{-1} . Figure 1

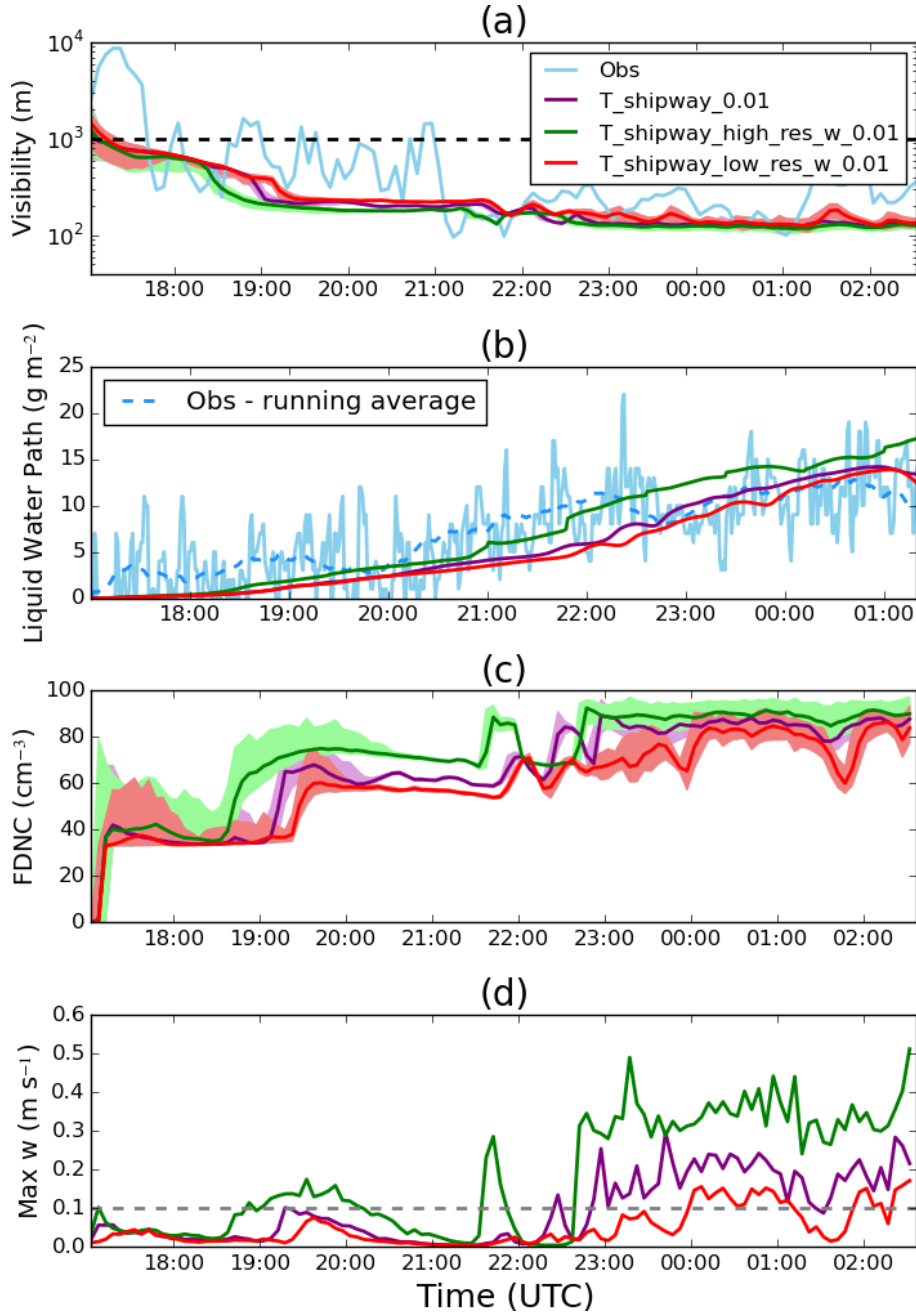


Figure 1: Time series of: (a) - mean visibility (m) at a 2 m altitude; (b) - the liquid water path ($g m^{-2}$); (c) - the mean CDNC (cm^{-3}) at a 2 m altitude; (d) - the maximum updraft velocity ($m s^{-1}$) at a 2 m altitude. Purple - $T_{shipway_0.01}$; green - $T_{high_res_wmin_0.01}$; red - $T_{high_res_wmin_0.01}$; light blue - observations of (a) near-surface visibility and (b) liquid water path respectively; black dashed line - fog threshold of 1 km ; grey dashed line - w_{min} threshold of $0.1 m s^{-1}$.

shows that increasing our horizontal resolution leads to an increase in both liquid water and FDNC, leading to the fog deepening faster. The increased resolution led to more resolved vertical motions and more activation. Therefore, it would be a suitable option for us to consider a higher resolution. However, running our case at a 1 m resolution led to both an increase in computational expense. In addition, the storage required to run all the simulations required for our study would mean that we could have run into further technical complications. Finally, our work shows that the relevant difference between activation scheme is greater than horizontal resolution. Therefore, by running all of our cases at a 2 m resolution, we feel that this is the best compromise to not alter the fog evolution too greatly and in addition, not compromise the conclusions that we made for our work.

Given these changes, we have changed the wording in our paper to the following:

”Although previous studies such as Maalick et al. (2016) and Maronga and Bosveld (2017) have run LES fog simulations at higher horizontal resolutions, we found that running our cases at 2 m although for us to address our objectives, whilst compromising on both data storage and computational expense (not shown).” This is located on lines 248-251.

7. This is one of my major concerns. Your paper is supposed to illustrate that the SMOD scheme gives a smoother/delayed transition to deep fog and thus is more realistic. But what is almost completely missing is evidence for this. First of all, you show the LANFEX observations, but you do not really compare your LES results against them. And what I see is actually, that all runs performed are way off from the observations. So how can you conclude that the SMOD scheme is more realistic? It appears a rather academic idea that is not proven by better agreement with observations for instance (you see rather bad agreement e.g in Figures 3, 5, and 7). Second, where can we see this smoother transition to deep fog? The longwave downwelling radiation is a good indicator. Looking at Figure 7, however, it looks like the fog layer in general remains less thick, no matter what scheme is used. The transitions, however, happen at the same time. And even worse: in the LES all runs go into deep fog mode quickly, while the observations indicate shallow fog or no fog until 21:00, and then a rapid thickening. I would say the Shipway scheme here is the only scheme given the same rapid jump; but at a different time and different radiation level.

Thank you for this feedback. The main objective of the paper is to show that using an aerosol activation scheme designed for convective clouds is unsuitable for modelling radiation fog. Hence why with our MONC simulations, we focused on changing w_{min} and understanding SMOD was sensitive to r_e . However, based on both reviewers 2 comments, we felt that addressed our original objectives too narrowly, consequently leading to our analysis not utilising the IOP1 observation dataset. With this in mind, with the evidence originally presented, SMOD did not appear to be the ideal represented for fog simulations. Given all of this reasoning, we have expanded both our analysis and discussion to address these concerns.

To begin, we firstly present a new analysis of the modelled to observed sensible heat flux (SHF), which can be located at Fig. 3b of our revised manuscript. For all our simulations, they are mostly zero or

slightly negative up until 2100 UTC, which agrees well with observations. After 2100 UTC, they all become more positive, with both T_SMOD and T_Shipway_wmin having the highest increase in SHF with time. With all of our simulations, SMOD with an increased r_e of 20 μm (T_SMOD_er_20) is closest to observations, despite it still being positive after 2100 UTC. This result indicates that T_SMOD_er_20 with the default settings being amended for a change in FDNC is the best option, even though the fog still grows too much in optical thickness in comparison to observations. Next, we have added new analysis which makes use of the vertical FDNC that was observed at different time frames throughout the night (Fig. 4 in the revised manuscript). We first note that for all the tests that run with just Shipway and SMOD in their default settings, they all have the deepest fog layers. In addition, T_SMOD and T_Shipway_wmin both have the highest proportion of modelled to observed fog droplets (see Table 6). T_Shipway_0.01 initially has the best spatial vertical variation when compared to observations. However, T_SMOD_er_20 appears to perform best in comparison to observations when all three-time frames are considered throughout the night. Finally, we have amended the figures and analysis to directly compare the SMOD and Shipway tests better. We believe it is now clearer that SMOD produced better results compared with the observations from the case study.

We note that throughout this study all of our tests either 1. don't capture the initial variation shown in specific diagnostics e.g. near-surface visibility (Fig. 3a of the original manuscript) or 2. transition to too deep of a layer too fast. As discussed in Poku et al. (2019), it was suggested that given that the way to better capture the fog's transition is to just use an aerosol activation scheme that accounted for more realistic physical processes. What our study has highlighted, however, is that there are potential discrepancies that we have not accounted for in terms of aerosol-fog interaction representation. For example, Schwenkel and Maronga (2020) discussed how the use of a bulk microphysics scheme can account for the condensation rate being too high, leading to too thick of a fog layer. We also note that there are studies that have addressed to account for processes such as nucleation scavenging when simulating aerosol-cloud interactions (e.g. Miltenberger et al., 2018). Given both of these examples may be of importance to our work, we have added this section into both our analysis and conclusions for this work.

In conclusion, we have highlighted that a scheme based on adiabatic cooling is wrong, and demonstrated the magnitude of the error this can introduce both offline and online. Our new scheme is therefore more physically realistic and we proposed that it should be adopted (in models such as NWP). However, we do not claim that this will solve all the problems with modelling fog onset and development, and indeed this is support by our more detailed comparison with the IOP observations.

8. line 382: with respect to my previous comment, I doubt that here is enough evidence for this.

Please refer to point 7, where we address this comment.

9. line 10: do you mean "initial fog droplet number concentration"?

We have amended this wording, which can be found on line 10 of our revised manuscript.

10. line 30-31:This sentence appears trivial for ACP and can be removed.

We have removed this sentence.

11. throughout text and equations: put index letters in non-italic font unless they are variables themselves

Thank you for this comment. We have gone through the manuscript and amended our index letters to be put into non-italic fonts.

12. line 154: "potentially"?!

We've changed this line in our revised manuscript to include the following: "and hence provide a potential solution for fog modelling that may require some form". This can be located on line 172.

13. Figure 1:label on y-axis for (a) should be s_{max} instead of S_{max} (to be in line with the nomenclature)

We have amended Fig. 1 to account for this change.

14. line 215: What is MONC?

We have included a description for MONC to include the following: "This section will investigate the impact that aerosol activation representation will have on fog evolution, using the Met Office Natural Environment Research Council Cloud (MONC) model (Brown et al., 2015, 2018). MONC is a large-eddy simulation model designed to research and develop parameterisations used in the forecast model. MONC and has the same equation set as the older Met Office Large Eddy Model (LEM; Gray et al., 2001) and unlike the LEM, MONC has been designed to couple with other modules, including the Cloud AeroSol Interactive Microphysics scheme (CASIM; Grosvenor et al., 2017; Miltenberger et al., 2018) and the Suite of Community Radiative Transfer codes (SOCRATES; Edwards and Slingo, 1996). MONC is widely used in the UK atmospheric science community, and has been used to study atmospheric processes in low level clouds in West Africa (Dearden et al., 2018), fog (Poku et al., 2019) and idealised convection simulations (Böing et al., 2019)." This can be located from lines 233-241.

2 Reviewer 2's comments and responses

1. The improvement brought by the SMOD scheme is not convincing, and it is a problem as it is the main objective of the paper. The authors argued a more realistic approach but it is a theoretical point of view. In fact there is no improvement for IOP1, and all the simulations show significant differences with the observations.

Thank you for your feedback. We do agree that this was the paper's main objective, however, our original manuscript was too narrow in both our analysis and discussion. Based on both yours and reviewer 1's comments, we have supported our argument by providing a more detailed comparison with IOP1 observations and expanded our discussion to account for highlighted discrepancies in our work. For a more detailed response, please refer to point 7. in Reviewer 1's comments.

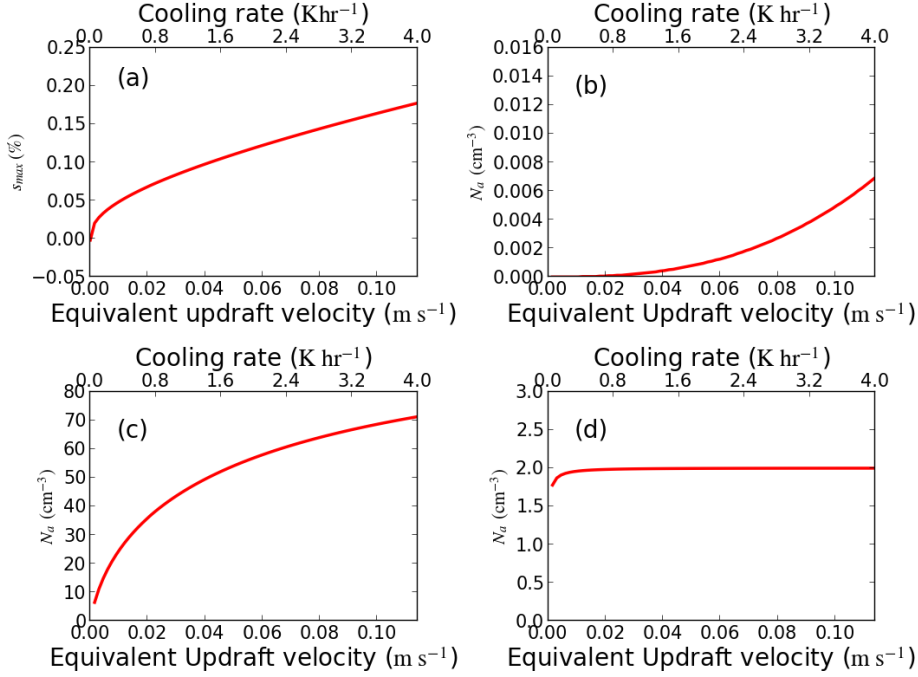


Figure 2: (a) Maximum supersaturation, s_{max} (%), against the total cooling rate for IOP1 assumed aerosol distribution with the Shipway scheme. (b) - (d) A plot of activated aerosol concentration, N_{act} (cm^{-3}) against the total cooling rate for Aitken, accumulation and coarse mode aerosols respectively for IOP1 assumed aerosol distribution.

2. The initialization of aerosol is chosen to limit the discrepancy with the observations but is not realistic, and not representative of the clean air typically found at Cardington. Indeed, direct observations of aerosol concentrations were not available for this case, but we can rely on typical measurements over Cardington. The authors would argue that the initialization of a single accumulation mode with 100 cm^{-3} has already been used in Poku et al. (2019) but it was already unrealistic. The reference paper for IOP1 for the time being is Boutle et al. (2018), who proposed an aerosol distribution initialised with 1000 cm^{-3} concentration of Aitken-mode aerosols, 100 cm^{-3} accumulation-mode aerosols and 2 cm^{-3} coarse-mode aerosols. Authors also argued that Aitken mode aerosol can be ignored, but they have to prove it by running a simulation with the 3 modes and the initial concentrations proposed by Boutle et al. (2018), and by comparing it with the present simulation. I am not at all convinced by this equivalence, and by the justification to neglect the Aitken mode. This comparison is required for the acceptance of the paper.

Thank you for your feedback. However, we believe that based on the assumed aerosol-size distribution used by Boutle et al. (2018), our key conclusions would not change. Figure 2a shows the change in s_{max} with cooling rate, with Figure's 2a showing the change in N_a with cooling rate for Aitken, accumulation and coarse mode aerosols respectively. Within the tested parameter space, the greatest proportion of N_a is within the accumulation mode. More specifically at the tested parameter's space maximum, accumulation mode N_a makes up 97.2% of the total aerosol population from the assumed aerosol activation

spectrum. In our paper, our results show that the changes in activation are stronger in the offline box model in comparison to MONC. Therefore, in the context of our study, it's unlikely that running MONC in a multi-mode setting would invalidate the presented results.

We acknowledge that in our work, there are some limitations in aerosol treatment due to MONC not having a prognostic for supersaturation and MONC using a bulk microphysics scheme to calculate condensation. In both of these instances using a multi-mode aerosol spectrum may be critical, which should be the subject for future work. We have added this argument to the paper's discussion section and included the following line in the methodology:

“With regards to aerosol sizes, only accumulation mode aerosol where $0.1 \mu\text{m} < \text{CCN size diameter} < 1 \mu\text{m}$) are accounted for. During IOP1, there were no direct aerosol or CCN measurements. Therefore, a CCN value of 100 cm^{-3} in the accumulation mode was set, with a total soluble mass of 2.7 ng throughout the initialised vertical profile and an assumed lognormal size distribution with a standard deviation of 2.0, based on typical measurements for a clean rural site similar to Cardington, UK (Boutle et al., 2018; Poku et al., 2019). Our simulations used a single aerosol mode to maintain consistency with the tests in the Shipway Box Model, which showed that when considering aerosol activation the activated N_a for IOP1 can be accounted for by accumulation mode aerosols (not shown). Therefore, we believe that using a multi-mode aerosol spectrum would have led to an unnecessary computational expense in this study. This reasoning may be different should these simulations have been run with a prognostic for supersaturation, however, this is outside the scope of this work.” This amendment can be found from lines 263-271.

3. In the same way, the fog life cycle is only presented during 10 hours, but it would be more interesting to present the whole life cycle until 12 UTC as in Boutle et al. (2018): we can indeed suppose that it is not shown as the simulations would depart too far from the observations.

Thank you for this suggestion. We agree that presenting the full life cycle to 12 UTC would have provided an interesting insight regarding different aerosol impacts on the fog evolution. At the time of this work being done, MONC was not coupled to an interactive land surface scheme. Given the discrepancies we found in our analysis of variables such as surface heat fluxes, we have focused on the earlier stages of fog develop. In addition, as we didn't have any aerosol measurements from IOP1 to compare with our study, this may have led to us coming to conclusions that do not necessarily correctly represent these impacts. Finally, despite using a more “realistic” aerosol activation scheme, our proposed set up doesn't capture features such as the fog variability correctly. This highlights the need to account for additional aerosol impacts, e.g. aerosol-radiation interactions, which would be key during the daytime phase of the fog cycle. Unfortunately, investigating these science areas are outside the scope of this work. To address this point, we have included the following in the conclusion of this paper:

“Finally, our study has focused on the first 10 hours of IOP1 and hence has not accounted for the fog evolution during daytime. Given the impact additional processes such as aerosol-radiation interactions and

interactive surface scheme will have on fog dissipation, it's critical to ensure schemes such as SOCRATES and CASIM are coupled for this future work." This addition can be located on lines 484-486.

4. Too few observations are used to evaluate the simulations: other temporal evolutions, for temperature, vertical velocity variances, sensible heat flux are available for this IOP, as well as vertical profiles of cloud mixing ratio, droplet concentration, droplet diameter. New comparisons need to be added in order to prove that SMOD is more realistic. They are also required for the acceptance of the paper.

Thank you for your feedback. We have compared our simulations to more available observations from IOP1 with the aim to demonstrate that unsuitability of using a scheme designed for convective clouds in fog modelling studies. We have addressed this concern in more detail in point 1 of your review and in point 7. in Reviewer 1's comments.

5. The study is not presented in a larger context where major papers have introduced some advances in the activation parametrization. Hence Thouron et al. (2012) for stratocumulus and Lebo et al. (2012) for deep convective clouds studied the relevance of saturation adjustment for LES. Then Schwenkel and Maronga (2019) studied the activation parametrization for LES of fog, but the authors only mention this last study in the conclusion. The necessity to consider the radiation cooling in the supersaturation evolution equation for fog is not new. So my general question is: what does this paper bring compared to the previous studies ? If new results are indeed shown, then they should be presented in the context of these other studies. It would be also necessary to compare the SMOD equations with the equations of Schwenkel and Maronga (2019) for instance.

Firstly, we would like to thank you for providing us with new literature that allowed us to put our work into the context of activation parameterisation studies. In addition to expanding both the introduction, analysis and discussion, we have clarified that our study is new in the sense that:

1. Although as suggested by Boutle et al. (2018) that the solution is to remove the w_{min} threshold when simulating radiation fog, our results show that this is not necessarily a suitable option. This is highlighted with T_shipway_0.01, which although did initially perform better than the rest of the tests discussed, it transitioned to a thicker fog than both T_SMOD_er_15 and T_SMOD_er_20. As aerosol activation in T_shipway_0.01 was driven by just an updraft velocity, this suggests why a more physical based activation scheme such as SMOD is critical to simulate nocturnal radiation fog. More specifically, the choice in activation scheme is key when the fog layer may transition to an optically thick layer.
2. Although there has been studies investigating the use of the non-adiabatic framework in fog simulations, this is the first study to the author's knowledge that critiques this framework with a fog case that formed in a clean aerosol regimes (accumulation $CCN < 100 \text{ cm}^{-3}$ as defined by Boutle et al., 2018), therefore supporting previous literature on the topic of aerosol-fog interactions.

We are aware that regarding SMOD, there are some limitations in the scheme e.g. the use of a bulk

microphysics scheme and not using a prognostic for supersaturation. However, given that our study focused on simulating a thin fog case, we feel that that it best highlights what missing physical processes are needed to be accounted for when simulating fog. In addition, whilst we've used LES in our work, the study was initially motivated to develop a new scheme suitable to be used in models such as NWP's. Therefore, we believe that we have been able to present a suitable option when looking to improve rural fog forecasts that are common in countries such as the UK. We have included these clarifications in the revised manuscript in both the Discussion and Conclusion section.

6. For the visibility calculation, why not to use a direct calculation according to the Koschmieder (1925) equation, linking the visibility to an extinction coefficient function of the DSD, through the Mie theory, instead of a diagnostic from Gultepe et al. (2006). (2006), which could be questionable?

Thank you for this comment. We believe that this is a good point and that it is something we are partly addressing in future with the use of the new VERA visibility diagnostic including aerosol effects, but it is beyond the scope of this work. In the revised manuscript this is only one aspect of the validation with observations, and since none of the simulations perfectly reproduce the observations we don't feel at a more accurate visibility calculation would alter the conclusions.

7. MONC needs to be presented.

Please refer to point 14 of Reviewer's 1 comments and responses.

8. 1 224-225 : the remark about the grid spacing is hardly understandable: why is it critical to run MONC at 1m or 2m resolution? The same sentence has been written in Poku et al. (2019) and it was already misunderstood.

Please refer to point 6 of Reviewer's 1 comments and responses.

9. The radiation scheme SOCRATES is called every 5 min. Is it not too large for a LES of radiation fog, with a necessary accurate estimation of radiative cooling ?

Thank you for pointing this out. Upon further inspection, it was found that SOCRATES was being called every 30 secs as opposed to every 5 mins, which was an error on our part. However, to check this value was sufficient, a test was run with SMOD which called for SOCRATES every 10 secs. Upon comparison, there was no appreciable difference between both runs (not shown).

We've corrected this mistake in the manuscript which can be found on line 252.

10. 1 254 : it is said that radiative cooling is the biggest source of saturation. But it would be nice to compare it to the total temperature tendency, or to show that the consideration of the turbulent contribution to the non-adiabatic temperature tendency does not change the results.

Thank you for this comment. When we were doing this study, we did consider how changes in subgrid mixing may be important for our simulations. In our work, we demonstrate that the total CDNC is

sensitive to the resolved updraft velocity’s strength. The strength of the resolved updraft velocity is determined by the model’s mixing scale length, λ_m , such that:

$$\lambda_m = c_s \times \max(\Delta x, \Delta y), \quad (1)$$

where c_s is the Smagorinsky constant and $\max(\Delta x, \Delta y)$ is the maximum grid box size in the horizontal. Any motions smaller than λ_m is calculated by the subgrid parameterisation, which can account for motions such as diffusion and small scale turbulent mixing.

Porson et al. (2011) discussed the importance of c_s on the fog layer’s development. They showed that reducing c_s and hence λ_m resulted in an increase level of TKE that was resolved, leading to the modelled boundary layer to deepen. Our work uses an aerosol activation scheme as opposed to a fixed droplet number used in the study by Porson et al. (2011), leading to the suggestion that the calculated CDNC is also sensitive to the levels of resolved TKE. Consequently, the initial fog formation may be more sensitive to the level of subgrid mixing, in addition to the change in sedimentation rate, as w_{min} is reduced.

To understand the impact of subgrid mixing on the formation and development of IOP1, we had a set of tests to understand how sensitive is the fog’s evolution to the choice in mixing length. We addressed this objective by changing the default c_s used in test T.shipway_0.01, by doubled and halved it to 0.46 and 0.115 respectively (default Smagorinsky constant is set to $c_s = 0.23$). Until 1900 UTC, there is no appreciable change in the near-surface visibility or LWP (Figure 3a). From 1900 UTC, increasing (decreasing) c_s results in an increase (decrease) in near-surface visibility. As the LWP is not appreciably different in these sensitivity tests (Figure 3b), the change in near-surface visibility is due to the amount of TKE being resolved, therefore directly impacting the maximum updraft velocity and hence CDNC (Figure 3d and c respectively). However, although the fog’s evolution shows a slight sensitivity to subgrid mixing, its development appears to be mostly driven by a change in sedimentation rate due to a decrease in w_{min} . Given these results, we are confident that although we’re not using the full non-adiabatic tendency, we are confident that our conclusions would not change in the revised manuscript. These figures have not been included in the revised manuscript.

11. 1 320 : there is a reference to the impact of surface heterogeneities, but it is not clear why this discussion is introduced here. Bergot et al. (2015) considered buildings, while Mazoyer et al. (2017) and Ducongé et al. (2020), which considered trees and orography (over Lanfex) heterogeneities respectively, could be added.

We introduced this discussion to show how processes such as nucleation scavenging may be critical to capture the fog’s spatial variability, which has been highlighted since using a more “realistic” aerosol activation scheme. We have clarified this sentence from line 375.

References

- Albrecht, B. A. (1989). Aerosols, cloud microphysics, and fractional cloudiness. *Science*, 245(4923):1227–1230.
- Bergot, T., Escobar, J., and Masson, V. (2015). Effect of small-scale surface heterogeneities and buildings on radiation fog: Large-eddy simulation study at Paris-Charles de Gaulle airport. *Quarterly Journal of the Royal Meteorological Society*, 141(686):285–298.
- Böing, S. J., Dritschel, D. G., Parker, D. J., and Blyth, A. M. (2019). Comparison of the Moist Parcel-in-Cell (MPIC) model with large-eddy simulation for an idealized cloud. *Quarterly Journal of the Royal Meteorological Society*, 145(722):1868–1881.
- Boutle, I., Price, J., Kokkola, H., Romakkaniemi, S., Kudzotsa, I., Kokkola, H., and Romakkaniemi, S. (2018). Aerosol-fog interaction and the transition to well-mixed radiation fog. *Atmos. Chem. Phys*, 18:7827–7840.
- Brown, N., Weiland, M., Hill, A., and Shipway, B. (2018). In situ data analytics for highly scalable cloud modelling on Cray machines. *Concurrency and Computation: Practice and Experience*, 30(1):e4331.
- Brown, N., Weiland, M., Hill, A., Shipway, B., Maynard, C., Allen, T., and Rezny, M. (2015). A Highly Scalable Met Office NERC Cloud Model. In *Proceedings of the 3rd International Conference on Exascale Applications and Software*, page 137. University of Edinburgh.
- Dearden, C., Hill, A., Coe, H., and Choularton, T. (2018). The role of droplet sedimentation in the evolution of low-level clouds over southern West Africa. *Atmos. Chem. Phys*, 18:14253–14269.
- Duongé, L., Lac, C., Vié, B., Bergot, T., and Price, J. D. (2020). Fog in heterogeneous environments: the relative importance of local and non-local processes on radiative-advective fog formation. *Quarterly Journal of the Royal Meteorological Society*, 146(731):2522–2546.
- Edwards, J. M. and Slingo, A. (1996). Studies with a flexible new radiation code. I: Choosing a configuration for a large-scale model. *Quarterly Journal of the Royal Meteorological Society*, 122(531):689–719.
- Gray, M. E. B., Petch, J., Derbyshire, S. H., Brown, A. R., Lock, A. P., Swann, H. A., and Brown, P. R. A. (2001). Version 2.3 of the Met. Office large eddy model. *Met Office (APR) Turbulence and Diffusion Rep*, 276.
- Grosvenor, D. P., Field, P. R., Hill, A. A., and Shipway, B. J. (2017). The relative importance of macro-physical and cloud albedo changes for aerosol-induced radiative effects in closed-cell stratocumulus: insight from the modelling of a case study. *Atmospheric Chemistry and Physics*, 17(8):5155–5183.
- Gultepe, I., Müller, M. D., Boybeyi, Z., Gultepe, I., Müller, M. D., and Boybeyi, Z. (2006). A New Visibility Parameterization for Warm-Fog Applications in Numerical Weather Prediction Models. *Journal of Applied Meteorology and Climatology*, 45(11):1469–1480.

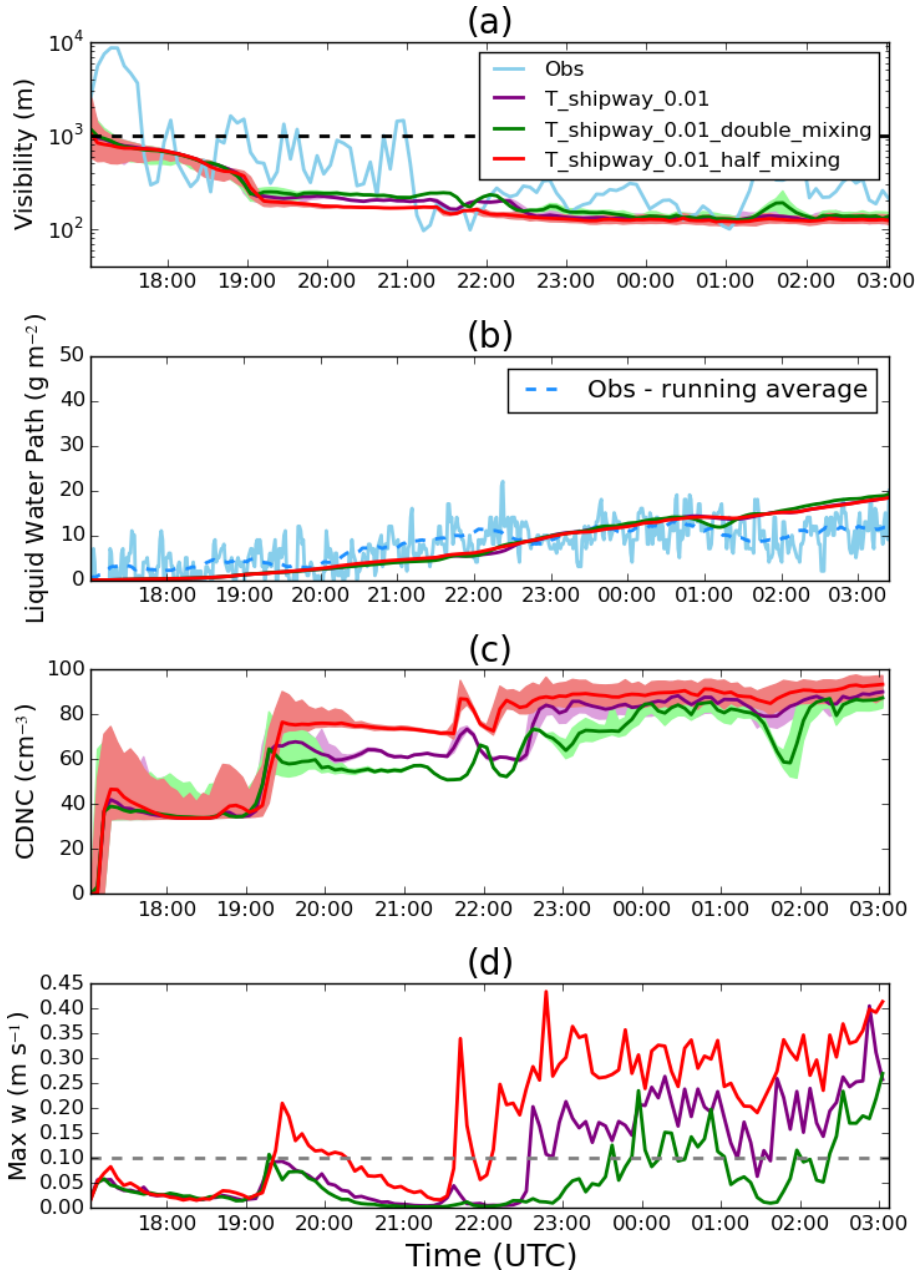


Figure 3: Time series of: (a) - mean visibility (m) at a 2 m altitude; (b) - the liquid water path ($g\ m^{-2}$); (c) - the mean CDNC (cm^{-3}) at a 2 m altitude; (d) - the maximum updraft velocity ($m\ s^{-1}$) at a 2 m altitude. Purple - $T_shipway_0.01$; green - $T_shipway_wmin_0.01_double_mixing$; red - $T_shipway_wmin_0.01_half_mixing$; light blue - observations of (a) near-surface visibility and (b) liquid water path respectively; black dashed line - fog threshold of 1 km ; grey dashed line - w_{min} threshold of $0.1\ m\ s^{-1}$.

- Lebo, Z. J., Morrison, H., and Seinfeld, J. H. (2012). Are simulated aerosol-induced effects on deep convective clouds strongly dependent on saturation adjustment? *Atmospheric Chemistry and Physics*, 12(20):9941–9964.
- Maalick, Z., Kühn, T., Korhonen, H., Kokkola, H., Laaksonen, A., and Romakkaniemi, S. (2016). Effect of aerosol concentration and absorbing aerosol on the radiation fog life cycle. *Atmospheric Environment*, 133:26–33.
- Maronga, B. and Bosveld, F. C. (2017). Key parameters for the life cycle of nocturnal radiation fog: a comprehensive large-eddy simulation study. *Quarterly Journal of the Royal Meteorological Society*, pages 2463–2480.
- Mazoyer, M., Lac, C., Thouron, O., Bergot, T., Masson, V., and Musson-Genon, L. (2017). Large eddy simulation of radiation fog: impact of dynamics on the fog life cycle. *Atmospheric Chemistry and Physics*, 17(21):13017–13035.
- Miltenberger, A. K., Field, P. R., Hill, A. A., Rosenberg, P., Shipway, B. J., Wilkinson, J. M., Scovell, R., and Blyth, A. M. (2018). Aerosol–cloud interactions in mixed-phase convective clouds – Part 1: Aerosol perturbations. *Atmospheric Chemistry and Physics*, 18(5):3119–3145.
- Poku, C., Ross, A. N., Blyth, A. M., Hill, A. A., and Price, J. D. (2019). How important are aerosol–fog interactions for the successful modelling of nocturnal radiation fog? *Weather*, pages 237–243.
- Porson, A., Price, J., Lock, A., and Clark, P. (2011). Radiation Fog. Part II: Large-Eddy Simulations in Very Stable Conditions. *Boundary-Layer Meteorology*, 139(2):193–224.
- Schwenkel, J. and Maronga, B. (2019). Large-eddy simulation of radiation fog with comprehensive two-moment bulk microphysics: impact of different aerosol activation and condensation parameterizations. *Atmospheric Chemistry and Physics*, 19(10):7165–7181.
- Schwenkel, J. and Maronga, B. (2020). Towards a Better Representation of Fog Microphysics in Large-Eddy Simulations Based on an Embedded Lagrangian Cloud Model. *Atmosphere*, 11(5):466.
- Thouren, O., Brenguier, J. L., and Burnet, F. (2012). Supersaturation calculation in large eddy simulation models for prediction of the droplet number concentration. *Geoscientific Model Development*, 5(3):761–772.
- Twomey, S. (1974). Pollution and the planetary albedo. *Atmospheric Environment (1967)*, 8(12):1251–1256.
- Whitby, K. T. (1978). The physical characteristics of sulfur aerosols. *Atmospheric Environment (1967)*, 12(1-3):135–159.

Is a more physical representation of aerosol activation needed for simulations of fog?

Craig Poku¹, Andrew N. Ross¹, Adrian A. Hill², Alan M. Blyth^{1,3}, and Ben Shipway²

¹School of Earth and Environment, University of Leeds

²Met Office, Exeter

³National Centre of Atmospheric Sciences, University of Leeds

Correspondence: Craig Poku (C.Y.A.Poku@leeds.ac.uk)

Abstract. Aerosols play a crucial role in the fog life cycle, as they determine the droplet number concentration, and hence droplet size, which in turn controls both the fog's optical thickness and life span. Detailed aerosol-microphysics schemes which accurately represent droplet formation and growth are unsuitable for weather forecasting and climate models, as the computational power required to calculate droplet formation would dominate the treatment of the rest of the physics in the model. A simple method to account for droplet formation is the use of an aerosol activation scheme, which parameterises the droplet number concentration based on a change in supersaturation at a given time. Traditionally, aerosol activation parameterisation schemes were designed for convective clouds and assume that supersaturation is reached through adiabatic lifting, with many imposing a minimum vertical velocity (e.g. 0.1 m s^{-1}) to account for unresolved sub-grid ascent. In radiation fog, the measured updrafts during initial formation are often insignificant, with radiative cooling being the dominant process leading to saturation. As a result, there is a risk that many aerosol activation schemes will overpredict the initial fog [droplet](#) number concentration, which in turn may result in the fog transitioning to an optically thick layer too rapidly.

This paper presents a more physically-based aerosol activation scheme that can account for a change in saturation due to non-adiabatic processes. Using an offline model, our results show that the [equivalent cooling rate associated with the](#) minimum updraft velocity threshold assumption can overpredict the droplet number by up to 70% in comparison to a [typical](#) cooling rate found in fog formation. The new scheme has been implemented in the Met Office Natural Environment Research Council (NERC) Cloud (MONC) LES model, and tested using observations of a radiation fog case study based in Cardington, UK. The results in this work show that using a more physically-based method of aerosol activation leads to the calculation of a more appropriate cloud droplet number. As a result, there is a slower transition to an optically thick (well-mixed) fog that is more in-line with observations.

The results shown in this paper demonstrate the importance of aerosol activation representation in fog modelling, and the impact that the cloud droplet number has on processes linked to the formation and development of radiation fog. Unlike the previous parameterisation for aerosol activation, the revised scheme is suitable to simulate aerosol activation in both fog and convective cloud regimes.

1 Introduction

25 Fog can be defined as a cloud at ground level with a surface visibility of less than 1 km (WMO, 1966). It can cause major disruption to road, aviation and marine transport, with associated economic losses that are comparable to those resulting from winter storms and hurricanes (Gultepe et al., 2007). Fog can have negative impacts on human health and the safety of certain activities. For example, thick fog on 5th September 2013 resulted in the Sheppey crossing crash in southeast England, consequently injuring 60 people (BBC, 2013). Understanding the physics behind fog is crucial in improving fog forecasting and mitigating the impact of such events.

~~A source of uncertainty in~~ An uncertainty within fog forecasting is ~~the representation of~~ caused by aerosol-fog ~~interactions.~~ ~~The Earth's atmosphere contains small suspended particles called aerosols, which range in size and composition~~ interaction representation (Pruppacher and Klett, 2010). Aerosols are important for both clouds and fog, as they act as the substrate on which water condenses and droplets form. The growth rate of these droplets is dependent on the initial aerosol size and solubility. The aerosols are considered to be 'activated' once these droplets reach a certain size, where they can grow more easily within a saturated environment (known as cloud condensation nuclei (CCN)). The aerosol population ~~has been shown to impact~~ is split by size categories. These size categories (hereafter known as modes) are technically defined as: the Aitken mode, where the diameter, d , of an aerosol particle is $< 0.1 \mu\text{m}$; the accumulation mode, where $0.1 < d < 1.0 \mu\text{m}$; and the coarse mode, where $d > 1.0 \mu\text{m}$ (Whitby, 1978). Due to their size, Aitken mode aerosols have an increased tendency to coagulate with other particles and not activate in their own right. In contrast, accumulation and coarse mode aerosols can activate into fog droplets, therefore indirectly impacting the cloud's microphysical structure and its life span (e.g. Twomey, 1974; Albrecht, 1989); ~~and these.~~ These impacts have been studied in great depth over the last few decades, both in the context of climate (e.g. IPCC, 2001) and meteorology (e.g. Seifert and Heus, 2013; Miltenberger et al., 2018). While research into radiation fog spans the last 100 years ~~(e.g. Taylor, 1917; Roach, 1976)~~ (e.g. Taylor, 1917; Roach et al., 1976), studies investigating aerosol impacts on fog are more recent. For example, Bott (1991) shows that aerosols fundamentally control ~~the optical thickness of radiation fog~~ radiation fog's optical thickness, and additional studies (e.g. Stolaki et al., 2015; Maalick et al., 2016) have verified ~~the importance of capturing the~~ why it's critical to correctly represent different aerosol indirect effects when simulating fog.

Accurate ~~representation of droplet nucleation~~ droplet nucleation representation, i.e. aerosol activation, is essential to represent the ~~indirect effects of aerosols~~ aerosol indirect effects on clouds. However, when investigating aerosol-cloud interactions in models such as general circulation models (GCMs) and numerical weather prediction (NWP) models, many detailed droplet growth schemes are unsuitable, as the computational power required would dominate the treatment of the rest of the physics in the model (Ghan et al., 1993). Original development of an aerosol activation parameterisation began by Squires (1958), with work by Twomey (1959) expanding on the modelling of aerosol activation. Twomey (1959) discussed the link between

an aerosol spectrum, supersaturation and droplet number concentration. Using Köhler Theory, Twomey (1959) formulated a parameterisation based on the change in supersaturation for a given time, such that:

$$\frac{ds}{dt} = \alpha - \beta s \int_0^s \nu(\sigma) \left[\int_{\tau(\sigma)}^t s dt \right]^{\frac{1}{2}} d\sigma, \quad (1)$$

where α is the ~~source of supersaturation due the cooling of a parcel~~ supersaturation source due to atmospheric cooling and the second term of Eq. (1) representing ~~the condensation of water vapour~~ water vapour condensation onto the activated aerosol population. The constant, β , is dependent on the aerosol spectrum, with $\nu(\sigma)\delta\sigma$ being the number of nuclei in a unit volume with critical supersaturation between σ and $\sigma + \delta\sigma$. As condensation results in a decrease in supersaturation, the maximum number of activated aerosols is capped and will occur once the peak supersaturation is reached (i.e. when the condensation term starts to dominate the cooling terms), resulting in no more aerosols activating. At this point, $\frac{ds}{dt} = 0$, and Eq. (1) becomes:

$$\alpha = \beta s \int_0^s \nu(\sigma) \left[\int_{\tau(\sigma)}^t s dt \right]^{\frac{1}{2}} d\sigma. \quad (2)$$

Different authors have addressed solving the right hand side of Eq. (2). Twomey (1959) formulated an upper and lower bound to the inner integral in Eq. (2) and assumed an aerosol spectrum, which was later developed further by Cohard et al. (1998), Shipway and Abel (2010) and Shipway (2015). Ghan et al. (1993) developed a scheme that accounted for a more realistic aerosol size distribution, which was naturally bounded by the total aerosol number. They showed that accounting for a more realistic single mode aerosol-size distribution (lognormal) improved the parameterised number of droplets activated. However, because droplet growth was neglected upon activation in their scheme, the introduction of multi-mode aerosol resulted in big discrepancies between the explicit and parameterised number of activated droplets. Work by Abdul-Razzak et al. (1998) (and later Abdul-Razzak and Ghan, 2000) combined the benefits of the parameterisations developed by both Twomey (1959) and Ghan et al. (1993). The scheme was not only bound by the total aerosol number, but also assumed that growth continued from the point of activation. The result of these assumptions led to the parameterised number of activated aerosols agreeing better with the explicit calculation for activation, even in regimes of high updraft velocities (Abdul-Razzak and Ghan, 2000). There has also been work to move away from using aerosol activation schemes in fog simulations using large eddy simulations. Recent work by Schwenkel and Maronga (2019) has shown that the choice in condensation calculation can be critical when investigating aerosol-fog interactions using large eddy simulations. More specifically, the same authors followed this study by demonstrating that using a bulk microphysics scheme in comparison to a lagrangian cloud model (LCM) can overestimate liquid water and inaccurately represent the fog droplet distribution (Schwenkel and Maronga, 2020). However, using methods such as LCMs is unsuitable for weather and climate models due to their massive computational expense.

So far, the ~~schemes discussed in this section~~ activation schemes discussed that are suitable for weather and climate models (i.e. Cohard et al., 1998; Abdul-Razzak et al., 1998; Abdul-Razzak and Ghan, 2000; Shipway, 2015) have been tested assuming

that saturation is driven by adiabatic ascent. In addition, a number of the listed schemes impose a fixed minimum updraft velocity threshold, w_{min} , of 0.1 m s^{-1} , corresponding to a cooling rate of 3.51 K hr^{-1} assuming a dry adiabatic lapse rate (e.g. Ghan et al., 1997; Abdul-Razzak and Ghan, 2000; Morrison and Gettelman, 2008; West et al., 2014). A w_{min} is suitable for these schemes, as they are designed to consider updrafts found in stratocumulus and convective clouds (Abdul-Razzak and Ghan, 2000; Meskhidze et al., 2005). Furthermore, some models (such as GCMs) will use the subgrid velocity (derived from the subgrid turbulence) to calculate the number of droplets. However, the turbulence driven by cloud-top radiative cooling can be poorly resolved above the planetary boundary layer (PBL) unless the model's vertical resolution was $< 100 \text{ m}$ (Ghan et al., 1997). Since such resolutions are not feasible in operational NWP or climate models, a w_{min} of 0.1 m s^{-1} is imposed to account for this unresolved turbulence (Ghan et al., 1997). In radiation fog, the main mechanism for the initial formation of droplets is radiative cooling; a non-adiabatic process, with measured cooling rates of $1 - 4 \text{ K hr}^{-1}$ at the surface (calculated using data from Price, 2011) and updraft velocities close to 0 m s^{-1} . Consequently, both the assumption of saturation being driven by adiabatic ascent, and the use of a minimum vertical velocity threshold do not accurately account for aerosol activation in fog (as discussed in Boutle et al., 2018). Finally, although there are studies that focus on investigating using a non-adiabatic framework in aerosol activation schemes when simulating fog (e.g. Zhang et al., 2014; Schwenkel and Maronga, 2019), there are no studies to the authors knowledge that test these assumptions for fog formation in clean aerosol regimes. Therefore, this may mean that using their schemes to simulate rural fog cases may lead to an overestimation in condensation (Shipway, 2015)

This paper will focus on addressing ~~both of these assumptions in~~ the assumptions using in activation scheme schemes to simulate fog with the modified Shipway (2015) ~~aerosol activation scheme~~. It was chosen to use Shipway over Abdul-Razzak and Ghan (2000) (hereafter referred to as ARG), as it has been shown that ARG overestimates condensation in low aerosol regimes, making it activate too few aerosols (Shipway, 2015). The work presented in this paper has been split into two sections: firstly comparing the original Shipway scheme (henceforth Shipway) with the modified Shipway scheme developed here (SMOD) using an offline box model, and secondly comparing both of these schemes using large eddy ~~simulation~~ simulations (LES) of an idealised fog case study (as described in Poku et al., 2019). During both comparisons, the following questions will be addressed:

1. What are the potential differences in aerosol activation between the Shipway and SMOD scheme?
2. How do the differences in aerosol activation representation impact on the fog evolution in a large eddy simulation?
3. What potential discrepancies are not account for when simulating aerosol-fog interactions?

Section 2 will present how the Shipway and SMOD scheme differ from each other mathematically. Section 3 will outline the Shipway box model setup and how the SMOD was implemented into it. Section 4 addresses research question 1. Section 5 describes the LES model used and addresses research question 2. A discussion and conclusion will then follow.

2 SMOD - Modifying the Shipway activation scheme to include non-adiabatic cooling

115 2.1 Shipway activation scheme

The Shipway (2015) aerosol activation scheme is designed as an improvement to the original lower bound approximation by Twomey (1959), and utilises a lookup table method that solves the maximum supersaturation at a reduced computational expense. Shipway assumes the differential activity spectrum, $\phi(s)$, to be lognormal, which can be expressed as:

$$\phi(s) = \sum_{i=1}^I \frac{N_i}{\sqrt{2\pi \ln(\sigma_{s,i})} s} \frac{N_i}{\sqrt{2\pi \ln(\sigma_{s,i})} s} \exp\left(-\frac{\ln^2(s/s_{0,i})}{\ln^2 \sigma_{s,i}} - \frac{\ln^2(s/s_{0,i})}{\ln^2 \sigma_{s,i}}\right), \quad (3)$$

120 where N_i is the number concentration of dry aerosol, $\sigma_{s,i}$ is the standard deviation of the distribution of $\phi(s)$, and $s_{0,i}$ is the mean geometric supersaturation for each given aerosol mode. Shipway (2015) formulated a new expression for the maximum supersaturation using the original Twomey (1959) lower bound approximation, such that:

$$\frac{\sqrt{2}\alpha^{\frac{3}{2}}}{\gamma} = s_{\max} \int_{s_{\max}}^{\infty} \phi(\sigma) \left[\frac{1}{2} \left(1 - \left(\frac{\sigma}{s_{\max}} \right)^{\mu} \right)^{\lambda} \right]^{-1} \left(s_{\max}^2 - \sigma^2 \right)^{\frac{1}{2}} d\sigma, \quad (4)$$

where μ and λ are chosen empirically by Shipway (2015) such that $\mu = 3$ and $\lambda = 0.6$. α relates to the increase in relative humidity and hence saturation, due to an air parcel undergoing atmospheric cooling. To date, the Shipway activation scheme assumes that α is driven by an updraft velocity, i.e.

$$\alpha = \psi(T, p) \frac{dz}{dt}, \quad (5)$$

where $\psi(T)$ is the thermodynamical function associated with a change in supersaturation and pressure due to adiabatic ascent, with:

$$130 \quad \psi = \frac{c_p}{R_a T} - \frac{L}{R_v T^2}, \quad (6)$$

L being the specific latent heat of vaporisation, and γ being a temperature pressure variable related to the change in temperature due to latent heat release, such that:

$$\gamma = \frac{p}{\epsilon e_s} + \frac{L^2}{R_v c_p T^2}. \quad (7)$$

Using a precalculated lookup table to solve the right-hand side of Eq. (4) and again s_{max} , Shipway (2015) calculates
 135 the total number of activated aerosols, N_{act} :

$$N_{act} = \frac{N_i}{2} \left[1 + \operatorname{erf} \left(\frac{\ln(s_{max}/s_{0,i})}{\sqrt{2} \ln \sigma_{s,i}} \right) \right], \quad (8)$$

with $\operatorname{erf}(x)$ being the error function (Abramowitz and Stegun, 1965). For the SMOD scheme (see Appendix A for further details), the term, α , in Eq. (4) has been modified to account for non-adiabatic cooling, such that:

$$\alpha = \psi_1 \left. \frac{dT}{dt} \right|_{ad} + \psi_2 \left. \frac{dT}{dt} \right|_{non_ad}, \quad (9)$$

140 where:

$$\psi_1 = \frac{c_p}{R_a T} - \frac{L}{R_v T^2}, \quad (10)$$

$$\psi_2 = -\frac{L}{R_v T^2}.$$

The SMOD scheme differs from Shipway when calculating N_{act} , in that it uses Eq. (9) to solve s_{max} (see Table A1 in Shipway, 2015, for a summary of terms described in this section and Appendix A for a full derivation of $\psi_{1,2}$). This term has also been used in previous studies such as Schwenkel and Maronga (2019) when investigating nocturnal radiation fog using LES.
 145

3 The Shipway box model - offline setup

To understand the flexibility of the SMOD scheme and how the thermodynamical function associated with the non-adiabatic contribution may impact N_{act} , both the Shipway and extended SMOD activation schemes will be directly compared using the Shipway box model (Shipway, 2015). The Shipway box model is designed as a non-interactive offline suite to calculate the
 150 initial number of activated aerosols in a range of different environmental settings. As the model is non-interactive, it permits analysis of parameter space, in the absence of atmospheric feedbacks. Inputs of the model are potential temperature, vertical velocity and aerosol population properties (number concentration, size, mode and distribution size parameters). Shipway (2015) used the box model to test the Shipway (2015) and Twomey (1959) activation schemes in different aerosol regimes, in addition to schemes developed by Abdul-Razzak and Ghan (2000) and Nenes and Seinfeld (2003).

155 For this work, the Shipway activation scheme was modified to account for a temperature change due to both adiabatic and non-adiabatic processes, using Eq. (9). Aerosol loadings from Whitby (1978) were used to test both activation schemes. These properties considered different environments, ranging from clean to polluted (Table 1). The temperature was set as a fixed

Table 1. Aerosol properties used to test the Shipway and SMOD schemes in the Shipway box model (Whitby, 1978).

Environmental setting	Distribution parameters	Aitken mode	Accumulation mode	Coarse mode
Marine	N (cm^{-3})	340	60	3.1
	σ	1.6	2.0	2.7
	r (μm)	0.005	0.035	0.31
Clean continental	N (cm^{-3})	1000	800	0.72
	σ	1.6	2.1	2.2
	r (μm)	0.008	0.034	0.46
Urban	N (cm^{-3})	10600	32000	5.4
	σ	1.8	2.16	2.21
	r (μm)	0.007	0.027	0.43

value of 274 K, based on surface temperatures observed during fog formation (Price, 2011; Haeffelin et al., 2013). All tests were driven by cooling rates found in fog formation ($1 - 4 \text{ K hr}^{-1}$ calculated using data from Price, 2011), and also accounted for a temperature change due to a nocturnal clear sky cooling ($0 - 1 \text{ K hr}^{-1}$; Kiehl and Trenberth, 1997).

Table ?? displays the setup of four cases: s 2 and 3 displays the case setups used in the offline box model, including the list of tests conducted in each case. Case C_adiabatic directly compared Table 2 lists all the tests that directly compared the Shipway and SMOD scheme, based on Eq.'s (4) and (9). Each scheme is tested with all combinations of the three different environments (marine, clean continental and urban) and the three different aerosol modes (Aitken, accumulation, coarse). To check that the SMOD scheme was correctly coded into the box model, meaning that supersaturation can be driven by a cooling rate rather than an updraft velocity, the non-adiabatic term in SMOD and w_{min} was set to zero. Conducting this case would also test the aerosol activation's sensitivity to the choice in aerosol mode, as well as testing how both Shipway and SMOD would behave with no w_{min} being present.

Case C_accumulation_mar aimed to understand the maximum impact that different aerosol activation representations may have on accumulation mode marine aerosols. Further cases (details in Table 3) were run in order to identify the impact of w_{min} in the Shipway scheme, and the impact of the non-adiabatic term in SMOD. For this case, three representations were used:

1. SMOD, which accounted for both adiabatic and non-adiabatic cooling. For these tests, $w_{min} = 0 \text{ m s}^{-1}$ and the adiabatic cooling component was switched off;
2. Default Shipway scheme. Cooling is assumed to be adiabatic, with $w_{min} = 0.1 \text{ m s}^{-1}$;
3. Shipway scheme, with cooling assumed to be adiabatic and $w_{min} = 0 \text{ m s}^{-1}$ (i.e. assuming no additional sub-grid cooling). This might be more appropriate for use in an LES where vertical motion is well resolved.

Table 2. The tests conducted in the offline box model [that directly compared Shipway and SMOD adiabatic mode based on Eq.'s \(4\) and \(9\).](#)

Case	Tests in case	Scheme used	Cooling source w_{min} applied -Aerosol mode	Environment
C_adiabatic_ship_ad_mar	T_ship_ad-mar_ait All-modes-T_ship_mar_acc T_ship_mar_coa	Shipway All-environments	Adiabatic-Aitken Accumulation Coarse	Marine
C_ship_ad_con	T_ship_con_ait T_ship_con_acc T_ship_con_coa	Shipway	Aitken Accumulation Coarse	Clean Continental
C_ship_ad_urb	T_ship_urb_ait T_ship_urb_acc T_ship_urb_coa	Shipway	Aitken Accumulation Coarse	Urban
C_SMOD_ad_mar	T_SMOD_mar_ait T_SMOD_mar_acc T_SMOD_mar_coa	SMOD	Adiabatic-Aitken Accumulation Coarse	Marine
C_SMOD_ad_con	T_SMOD_con_ait T_SMOD_con_acc T_SMOD_con_coa	SMOD	Aitken Accumulation Coarse	Clean Continental
C_SMOD_ad_urb	T_SMOD_urb_ait T_SMOD_urb_acc T_SMOD_urb_coa	SMOD	Aitken Accumulation Coarse	Urban

180 Firstly, a comparison between Shipway with no w_{min} and Shipway in its default setting (with an applied $w_{min} = 0.1 \text{ m s}^{-1}$) tested the suitability of a w_{min} in fog modelling. This comparison was motivated by Boutle et al. (2018), who discussed how aerosol activation in fog can be overestimated by the use of an [applied a \$w_{min}\$ value designed for convective clouds](#). The results of this test will quantify this overestimation, and hence provide [potential a solution guidance on how \$w_{min}\$ may require modification](#) for fog modelling ~~that may require some form of a w_{min}~~ . Next, a comparison between SMOD and Shipway with $w_{min} = 0 \text{ m s}^{-1}$ tested the suitability of assuming adiabatic cooling in a non-adiabatic environment.

185 ~~C_accumulation_mar was repeated for a clean continental and urban environment (test's C_accumulation_con and C_accumulation_urb respectively) to understand how the aerosol activation representation impacts may change based on the environment choice.~~

Table 3. The tests conducted in the offline box model used to test activation scheme representation and appropriate use of w_{min} .

<u>Case</u>	<u>Tests in case</u>	<u>Scheme used</u>	<u>Cooling source</u>	<u>w_{min} applied</u>	<u>Aerosol mode</u>	<u>Environment</u>
C_accumulation_mar	T_ship_mar_acc	Shipway	Adiabatic		Accumulation	Marine
	T_ship_mar_acc_wmin	Shipway	Adiabatic	x		
	T_SMOD_mar_acc	SMOD	Non-adiabatic			
C_accumulation_con	T_ship_con_acc	Shipway	Adiabatic		Accumulation	Clean continental
	T_ship_con_acc_wmin	Shipway	Adiabatic	x		
	T_SMOD_con_acc	SMOD	Non-adiabatic			
C_accumulation_urb	T_ship_urb_acc	Shipway	Adiabatic		Accumulation	Urban
	T_ship_urb_acc_wmin	Shipway	Adiabatic	x		
	T_SMOD_urb_acc	SMOD	Non-adiabatic			

4 Testing Shipway and SMOD using an offline box model

4.1 ~~C_adiabatic-behaviours~~ Behaviours of the Shipway and SMOD scheme in low updraft velocity regimes

~~The objective of C_adiabatic-~~ This section's objective is to understand the relative importance of different aerosol modes concerning aerosol activation in fog and to check that the adiabatic pathway in the SMOD scheme was coded correctly. Although the implementation for SMOD is different in that it applies a cooling rate rather than an updraft velocity, these tests comparing Shipway to SMOD should produce identical results for a given equivalent cooling rate.

When comparing the code that would control the adiabatic pathways in the Shipway and SMOD scheme, the differences in numerical calculations ~~agree~~ are negligible across all tests, which is shown by the overlapping dashed line over the solid line for all tests in Fig. 1. Figure 1a shows a monotonic increase in the maximum supersaturation, ~~s_{max}~~ s_{max} , across all environments with respect to updraft velocity. For a fair comparison, an equivalent cooling rate was calculated for the SMOD scheme using the dry adiabatic lapse rate assumption (see Eq. A6 in Appendix A). The ~~s_{max}~~ s_{max} is 0.26% for the marine environment; corresponding to a cooling rate of 4 K hr^{-1} , and decreases as the aerosol concentration increases (0.11 and 0.04% for the clean continental and urban environment respectively). The decrease in ~~s_{max}~~ s_{max} with increases in aerosol concentration relates to an increased competition of water vapour and hence condensation rate, resulting in a reduced likelihood of newly activated droplets.

Figures 1b-d show an increase in activated aerosols in relation to cooling rate. Of the three modes, the proportion of activated aerosols is greatest in the accumulation mode in all tested environments. This is even though in some environments (e.g. marine), the proportion of aerosol in the Aitken mode is greater than the accumulation mode (see Table 1). The relatively small radii of Aitken mode aerosol compared to the rest of the aerosol spectrum makes the required maximum supersaturation for activation significantly higher, as displayed in Fig. 1b. The reality is that supersaturation levels in fog have been shown to

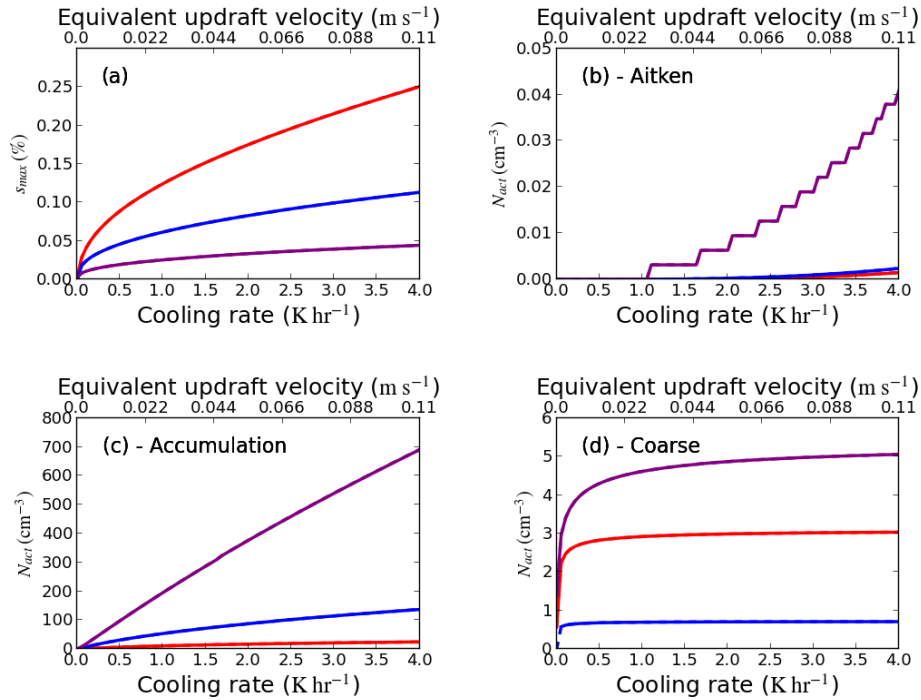


Figure 1. (a) Maximum supersaturation, s_{max} (s_{max} (%)), against the total cooling rate. (b) - (d) A plot of activated aerosol concentration, N_{act} (N_{act} (cm⁻³)) against the total cooling rate for Aitken, accumulation and coarse mode aerosols respectively. Red - marine; Blue - clean continental; Purple - urban. Solid line - T_ship_ad; Dashed line - T_SMOD_ad (solid line overlaying the dashed line).

only reach several tenths of 1% (Gerber, 1991), and hence would not be great enough to activate Aitken mode aerosol. Given the result of this test, it could indicate that nocturnal fog simulations that account for aerosol activation ~~could~~ can neglect the Aitken mode. This will be discussed further in Section 5. Although there is an increase in N_{act} (N_{act}) with respect to updraft velocity for Aitken mode aerosol (Fig. 1b), the aerosol activation fraction is so small that it leads to a visible stepwise function (this being strongest in the urban environment). The stepwise behaviour for the Aitken mode is a result of poor resolution in the look-up table for the Shipway scheme at low updraft velocities, where this behaviour has been highlighted due to w_{min} not being present. The resolution could be improved by using a more robust integration method. However, changing the integration method does not impact the general conclusions relating to the new scheme and hence this will be explored in later work.

4.2 Associated percentage difference for methods of aerosol activation

215 To understand how N_{act} (N_{act}) may be impacted by the choice in aerosol activation representation, accumulation mode tests ~~in C_adiabatic~~ displayed in Table 3 were rerun using the SMOD activation scheme and the Shipway (2015) scheme with an applied w_{min} . Although these same tests were run for Aitken and coarse mode aerosol (see Table 1), there was little to no change in N_{act} (N_{act}) when the aerosol activation representation was changed (not shown). In case C_accumulation_mar,

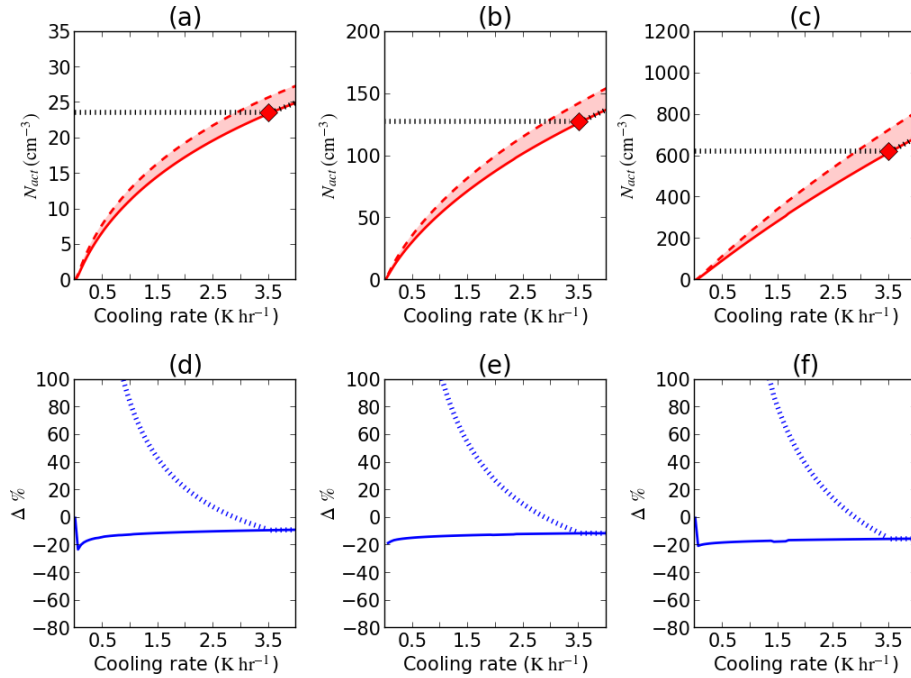


Figure 2. (a) Total activated aerosols, N_{act} , against the cooling rate for marine environment accumulation mode aerosols. Solid line - T_ship_mar_acc; dashed line - T_SMOD_mar_acc; black dashed line - T_ship_mar_acc_wmin. (d) Percentage differences, $\Delta \%$, between: dashed line - T_ship_mar_acc against T_ship_mar_acc_wmin; solid line - T_ship_mar_acc against T_SMOD_mar_acc. Red diamond - $w_{min} = 0.1 \text{ m s}^{-1}$ (b), (e): clean continental; (c), (f): urban.

T_SMOD_mar_acc produces a higher N_{act} than T_ship_mar_acc for all cooling rates (Fig. 2a - marine), with a similar pattern being applicable to the clean continental and urban environments (Figs. 2b and c). As the SMOD scheme for these tests
 220 assumes non-adiabatic cooling exclusively, the increase in N_{act} is due to the associated thermodynamical function being independent of adiabatic lifting and hence a change in pressure (see Appendix A for further details). Therefore, this demonstrates the dependency on the total number of activated aerosols on the way in which the cooling is applied. To understand the impact of a w_{min} threshold on N_{act} , all tests using the Shipway activation scheme were rerun, with the w_{min} threshold
 225 of 0.1 m s^{-1} being applied (Tests T_ship_mar_acc_wmin, T_ship_con_acc_wmin and T_ship_urb_acc_wmin). Applying this threshold resulted in a fixed N_{act} for a cooling rate below 3.51 K hr^{-1} . Consequently, should there be a cooling rate lower than this threshold, N_{act} will be overestimated and this may impact properties of the fog evolution such as the fog's optical depth.

Figures 2d, e and f show the percentage difference between the SMOD and Shipway (with an applied w_{min}) activation
 230 schemes increases as the prescribed cooling rate decreases. When comparing the three environments, the rate of increase in the percentage difference grows, as the tested environment becomes more polluted. For example, a cooling rate of 1.5 K hr^{-1} results in a percentage difference of 40, 50 and 70% for the three environments respectively. Given the associated percentage

235 difference, this indicates aerosol activation in fog simulations is overestimating N_{act} by an appreciable amount. However, reducing the minimum threshold, w_{min} , to give an equivalent cooling rate close to those observed in fog would reduce but not remove the problem associated with the percentage difference. Between the SMOD and Shipway schemes for aerosols in the accumulation mode, the associated percentage change ranges between -10 and -20% for all three environments, and the rate of change in the percentage difference is not appreciably different for any given environment (Figs. 2d, e and f). This implies that even if the minimum threshold of w_{min} were to be reduced such that it is representative for updraft velocities found in radiation fog, just using the Shipway scheme could potentially underestimate aerosol activation.

240 5 Testing Shipway and SMOD using MONC

The offline box model results demonstrate that assumptions widely used in aerosol activation (e.g. Abdul-Razzak and Ghan, 2000) may be significantly overestimating aerosol activation in fog. ~~In this section, the impact of this overestimation on fog development in~~ This section will investigate the impact that aerosol activation representation will have on fog evolution, using the Met Office Natural Environment Research Council Cloud (MONC) model (Brown et al., 2015, 2018). MONC is a large-eddy ~~simulations of fog is assessed using MONC~~ simulation model designed to research and develop parameterisations used in the forecast model. MONC and has the same equation set as the older Met Office Large Eddy Model (LEM; Gray et al., 2001) and unlike the LEM, MONC has been designed to couple with other modules, including the Cloud AeroSol Interactive Microphysics scheme (CASIM; Grosvenor et al., 2017; Miltenberger et al., 2018) and the Suite of Community Radiative Transfer codes (SOCRATES; Edwards and Slingo, 1996). MONC is widely used in the UK atmospheric science community, and has ~~been used to study atmospheric processes in low level clouds in West Africa (Dearden et al., 2018), fog (Poku et al., 2019) and idealised convection simulations (Böing et al., 2019). These tests have two objectives. The first objective is assessing the impact the assumption $w_{min} = 0.1 \text{ m s}^{-1}$ has on the simulated fog. The second objective is to understand how the SMOD scheme for aerosol activation impacts on the fog evolution and the causes of differences from the Shipway scheme.~~

5.1 MONC model - online setup

255 As part of this work, MONC is used to perform a suite of sensitivity tests based on intensive observation period 1 (IOP1) from the recent Local And Non-local Fog EXperiment (LANFEX) field campaign (Price et al., 2018). A full description of IOP1 and the observed vertical profiles the model was initialised with, can be found in Poku et al. (2019). The model setup for IOP1 is presented in Table 2.4. A domain size of $132 \times 132 \text{ m}^2$ was chosen, as there is minimal impact on the fog's turbulent kinetic energy (TKE) and liquid water when compared to simulations that were tested on a larger domain (not shown). ~~The choice of grid spacing was motivated by~~ Although previous studies such as Maalick et al. (2016) and Maronga and Bosveld (2017) ~~, which both show the fog formation's sensitivity to the model resolution. Therefore, it was critical to run MONC at such a high resolution~~ have run LES fog simulations at higher horizontal resolutions, we found that running our cases at 2 m allowed for us to address our objectives, whilst compromising on both data storage and computational expense (not shown). The model's surface boundary conditions were prescribed with a varying surface temperature (described in Poku et al., 2019)

Table 4. The input parameters and model setup for IOP1 in MONC.

IOP1 input parameters	Values
Horizontal domain	132 x 132 m
Vertical domain	705 m
$\Delta x, \Delta y$	2 m
Δz	Variable - 1 m first 100 m, stretched up to 6 m afterwards
Simulation duration	12 hr
Timestep	0.1 s
Surface geostrophic winds	$u_g = 1.3 \text{ m s}^{-1}, v_g = 2.1 \text{ m s}^{-1}$
Cloud microphysics	Cloud AeroSol Interactive Microphysics (CASIM)
Radiative transfer scheme	Suite of Community RAdiative Transfer codes (SOCRATES) (Edwards and Slingo, 1996)

265 and a surface vapour mixing ratio of 0.004 kg kg^{-1} , which were both based on observations. Radiation was calculated using ~~the Suite of Community RAdiative Transfer codes (SOCRATES)~~, SOCRATES based on the work of Edwards and Slingo (1996). SOCRATES was called by the MONC model every ~~5 min~~30 secs, allowing for the longwave radiative fluxes at the top of the fog layer to be captured in the model.

All simulations use the ~~Cloud AeroSol Interactive Microphysics (CASIM)~~ CASIM scheme; a multi-moment bulk micro-
 270 physics scheme designed to simulate aerosol-cloud interactions (Grosvenor et al., 2017; Dearden et al., 2018; Miltenberger et al., 2018). For this work, CASIM has been set to 2 moments and is being used to represent a non-precipitating, warm boundary layer cloud (i.e. ice processes and autoconversion to rain are turned off). In CASIM, the cloud-drop size distribution, $N(D)$, assumes a gamma distribution, which has the form (Shipway and Hill, 2012):

$$N(D) = N_0 D^{\mu_d} e^{-\lambda_d D}, \quad (11)$$

275 where N_0 is the distribution intercept parameter, μ_d is the shape parameter (the default value of μ_d is set to 0), λ_d is the slope parameter and D is the droplet diameter. For this work, μ_d has been set to equal 3.0, based on observations of the liquid water path (LWP) and cloud-drop size distribution during IOP1, resulting in a more sensible modelled sedimentation rate (see Appendix B for details). With regards to aerosol sizes, only accumulation mode aerosol where $0.1 \mu\text{m} < \text{CCN size diameter} < 1 \mu\text{m}$) are accounted for, ~~as at the time of development, MONC was unable to run with a multi-mode aerosol setting. Aerosol activation is being represented using both the original Shipway scheme and the new modified SMOD scheme.~~

280 During IOP1, there were no direct aerosol or CCN measurements. Therefore, a CCN value of 100 cm^{-3} in the accumulation mode was set, with a total soluble mass of 2.7ng throughout the initialised vertical profile and an assumed lognormal size distribution with a standard deviation of 2.0, based on typical measurements for a clean rural site similar to Cardington, UK (Boutle et al., 2018; Poku et al., 2019). Our simulations used a single aerosol mode to maintain consistency with the tests in

Table 5. Details of the simulations using the Shipway and SMOD activation scheme. The value of w_{min} has been lowered from 0.1 to 0.01 m s^{-1} based on the results from Sec. 4. Cooling rate equivalent calculated using the dry adiabatic lapse rate assumption.

Test no.	Test name	Scheme	Imposed w_{min} (m s^{-1})	Threshold cooling rate equivalent (K hr^{-1})	r_e (μm)
T1	T_shipway_wmin	Shipway	0.1	3.51	10
T2	T_shipway_0.01	Shipway	0.01	0.351	10
T3	T_SMOD	SMOD	N/A	N/A	10
T4	T_SMOD_er_15	SMOD	N/A	N/A	15
T5	T_SMOD_er_20	SMOD	N/A	N/A	20

285 [the Shipway Box Model](#), which showed that when considering aerosol activation the activated N_a for IOP1 can be accounted for by accumulation mode aerosols (not shown). Therefore, we believe that using a multi-mode aerosol spectrum would have led to an unnecessary computational expense in this study. This reasoning may be different should these simulations have been run with a prognostic for supersaturation, however, this is outside the scope of this work. To reduce computational expense and data storage, 1D diagnostics are output every 1min and 3D diagnostics are output every 5min.

290 SMOD was implemented into MONC based on Eq. (9), which involves adding the adiabatic and non-adiabatic contributions together for the combined cooling rate to them be used for aerosol activation. The adiabatic contribution for this equation was derived from the resolved positive updraft velocity in MONC. The non-adiabatic contribution to date only consists of the longwave heating tendency that is derived using SOCRATES. For reference, the implementation of these partitioned terms is done similarly to the aerosol activation scheme used by Vie et al. (2016). Although it has been acknowledged that there are
 295 other non-adiabatic contributions to changes in supersaturation such as turbulent mixing, further model development would be required to account for these changes. However, given that radiative cooling is the biggest source of saturation during fog formation (Roach, 1976)(Roach et al., 1976), these results should provide useful insight into the representation of aerosol activation during a stable fog case.

Table ??-5 displays all tests that will evaluate Shipway against SMOD. The first objective will be addressed by comparing
 300 test's T1 - T3, and outcome of this comparison will [result in a clear improved the](#) understanding of how different activation representations could influence the [cloud-fog](#) droplet number concentration ([CDNCFDNC](#)) evolution in IOP1. To date, the effective radius, r_e , has the option to be fixed or for it to vary with a change in [CDNCFDNC](#). In order to isolate the impact of aerosol activation on number concentration, this work used a fixed r_e . As the non-adiabatic contribution in the SMOD scheme is directly influenced by r_e , two tests were setup testing its sensitivity, and hence will motivate future work that involves
 305 deciding whether a coupled effective radius is required when using the SMOD scheme.

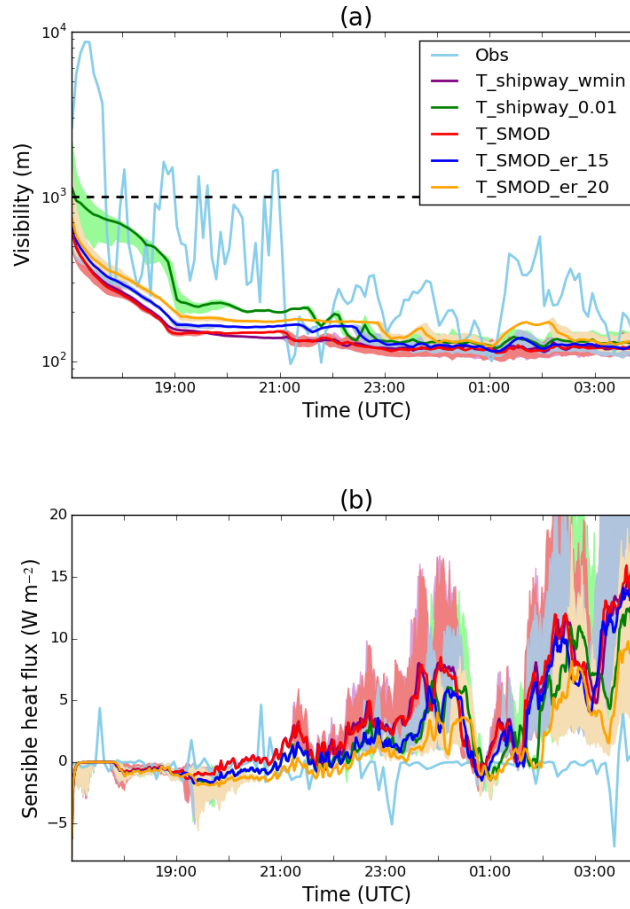


Figure 3. (a) - Time series of the near-surface mean visibility (Vis ; m) at a 2 m altitude. Purple – $T_{shipway_wmin}$; green – $T_{shipway_0.01}$; red – T_{SMOD} ; blue – $T_{SMOD_er_15}$; orange – $T_{SMOD_er_20}$; light blue – observations. Minimum and maximum visibility are marked on the figure by the shaded area. (b) - Time series of the liquid-water-path-surface sensible heat flux ($g\ W\ m^{-2}$). Purple – $T_{shipway_wmin}$; green – $T_{shipway_0.01}$; red – T_{SMOD} ; light blue – observations; blue – $T_{SMOD_er_15}$; orange – $T_{SMOD_er_20}$; light blue dashed – running average over observations. Minimum and maximum (40 points) visibility and (b) sensible heat flux are marked on the figure by the shaded area.

5.2 Comparing simulations using the Shipway and SMOD scheme

Fog forms in tests $T_{shipway_wmin}$, $T_{shipway_0.01}$ and T_{SMOD} at 1700 UTC, and all decrease to a mean near-surface visibility of 120 m by the end of the night (Fig. 3a). For all model simulations, visibility, Vis , is calculated using the formula of Gultepe et al. (2006):

$$310 \quad Vis = \frac{1.002}{(LWC \times CDNC)^{0.6473}} \frac{1.002}{(LWC \times FDNC)^{0.6473}}, \quad (12)$$

where LWC is the liquid water content and ~~$CDNC$ is the cloud~~ $FDNC$ is the fog droplet number concentration. Equation (12) was derived based on observations of fog in mainland Europe and is valid over a range of ~~$CDNC$ droplet concentrations~~ from a few per cubic centimetre up to a few hundred per cubic centimetre (Gultepe et al., 2006).

Despite the differences in near-surface visibility, all three tests have the strongest rate of decrease between 1700 and 1845
315 UTC (Fig. ~~??~~3a). During this time, the mean near-surface visibility in T_shipway_wmin, T_shipway_0.01 and T_SMOD decrease to 208, 151 and 210 m respectively. ~~However,~~ T_shipway_0.01 has a noticeably higher near-surface visibility before 1830 UTC and best agrees with observations, before decreasing in visibility at the same rate as T_shipway_wmin. Upon first inspection, it appears that just lowering w_{min} is the solution to prevent the simulation overestimating aerosol activation in fog, as shown by T_shipway_0.01. However, the model's spin-up period lasted around an hour in these simulations, meaning that
320 the ~~$CDNC$ $FDNC$~~ calculation is likely being influenced by initial prescribed random perturbations, as opposed to turbulence driven by either wind shear or convective motion. Unfortunately, with the earliest radiosonde data available being at 1700 UTC, the features in T_shipway_0.01 could not be avoided (for context, the observations show a stable boundary layer (SBL) beginning to form around the time of model initialisation). Nonetheless, the lower threshold used in T_shipway_0.01 allows for the simulation to undergo a slower transition in near-surface visibility to a thicker fog. This suggests that the number of
325 activated droplets calculated may account for inaccurate representation of what was observed during IOP1.

Up until 2100 UTC, T_shipway_wmin and T_SMOD and T_shipway_0.01 mostly experience a zero or slightly negative sensible heat flux (SHF), which agrees well with observations (Fig. 3b). After 2100 UTC, all three simulations grow positively in SHF, with both T_shipway_wmin and T_SMOD experiencing two distinct maxima of 6 and 14 W ms⁻² at times 0000 and 0400 UTC respectively. A mostly positive SHF is due to the fog layer growing enough in both depth and optical thickness that it will begin to warm the surface (Price, 2011). As the observed SHF was mostly zero throughout the night, our results indicate that the default w_{min} used in the Shipway scheme will lead to the fog episode transitioning to a well-mixed layer too quickly. Up until 0100 UTC, T_shipway_0.01 has a lower SHF than T_shipway_wmin and T_SMOD, despite it still remaining positive. This result highlights the inaccuracy of simulating fog cases with just an updraft velocity, providing further evidence for the use of the SMOD scheme. However, despite this suggestion, T_SMOD in its default settings is performing worse
330 than T_shipway_0.01. This discrepancy will be discussed further in Section 5.2.1 of this paper. There is a possibility that the simulated SHF results may have some uncertainty due to no land-surface scheme being coupled to MONC to date, which has been shown to be important when the fog becomes optically thick (e.g. Porson et al., 2011). Unfortunately, investigating this uncertainty is outside the scope of this work.

Vertical profiles of observed fog droplet number concentration (FDNC) initially show spatial variation throughout the layer, where it begins to homogenise throughout the night (Fig. 4). At 0030 UTC, it appears as though the fog layer decreased in height. However, this feature is most likely due to an instrumentation limitation, resulting in only accounting cloud droplets that were of sizes between 2 and 40 μm in diameter, with a 1 μm uncertainty (Price et al., 2018). Therefore, there is a potential that droplets that have begun growing through condensation were not accounted for. Within the fog layer, T_shipway_wmin and T_SMOD both have an activation rate between 75-80%, which increases to around 90% later in the night. Furthermore,
345 the modelled to observed fog droplets for both simulations is 2.77 and 3.03 respectively (Table 6). Consequently, both the

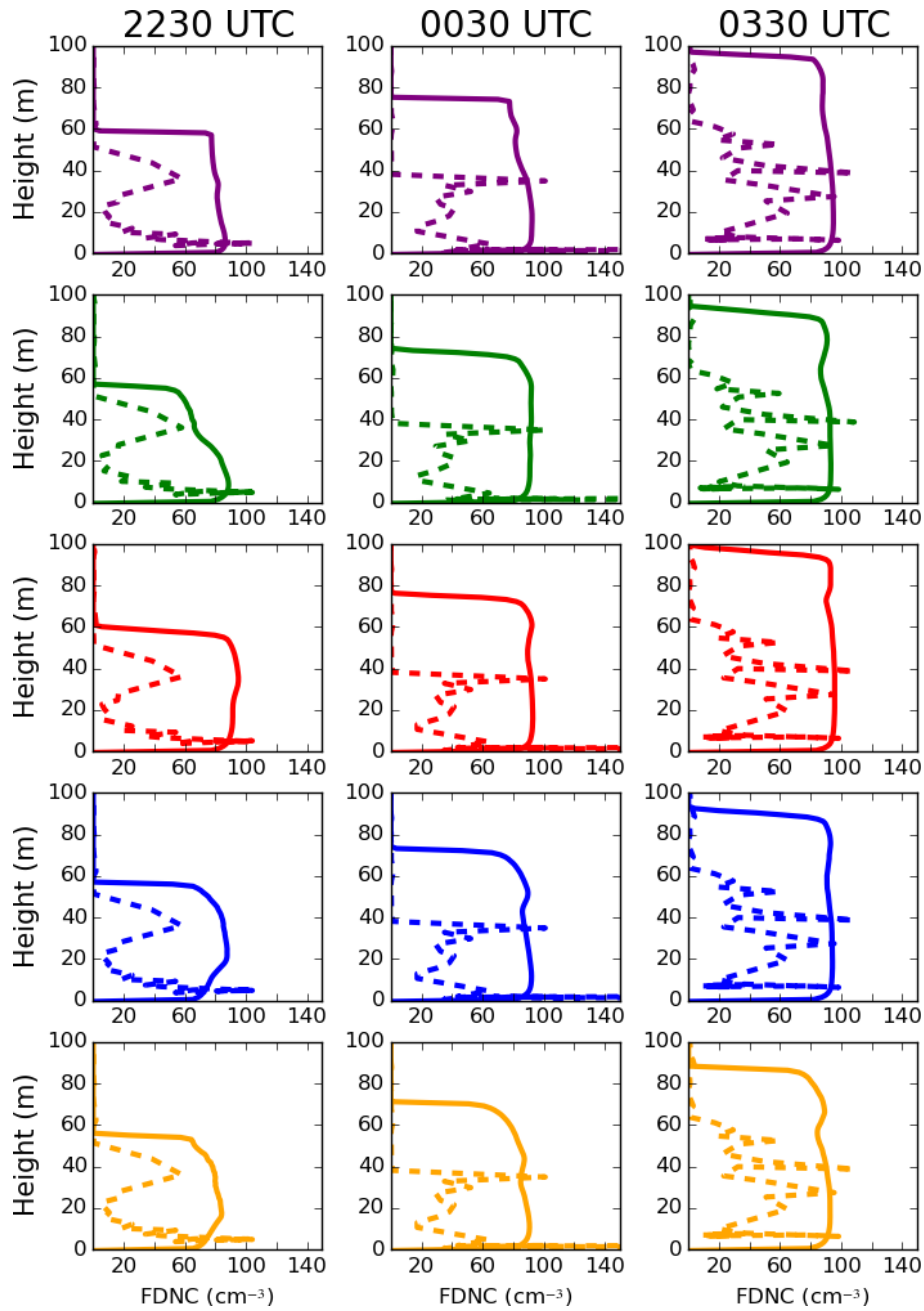


Figure 4. Vertical profiles of the fog droplet number concentration (cm^{-3}) at 2230, 0030 and 0330 UTC. The dashed lines represent observations, and solid lines represent simulated values. Purple – T_shipway_wmin; green – T_shipway_0.01; red – T_SMOD; blue – T_SMOD_er_15; orange – T_SMOD_er_20.

Table 6. Ratio of modelled to observed cloud drop number averaged over the vertical height across tested time frames (3 sf).

<u>Test name</u>	<u>2230 UTC</u>	<u>0030 UTC</u>	<u>0330 UTC</u>
<u>T_shipway_wmin</u>	<u>2.77</u>	<u>1.66</u>	<u>2.99</u>
<u>T_shipway_0.01</u>	<u>2.54</u>	<u>1.69</u>	<u>2.96</u>
<u>T_SMOD</u>	<u>3.03</u>	<u>1.70</u>	<u>3.07</u>
<u>T_SMOD_er_15</u>	<u>2.78</u>	<u>1.65</u>	<u>3.00</u>
<u>T_SMOD_er_20</u>	<u>2.63</u>	<u>1.59</u>	<u>2.92</u>

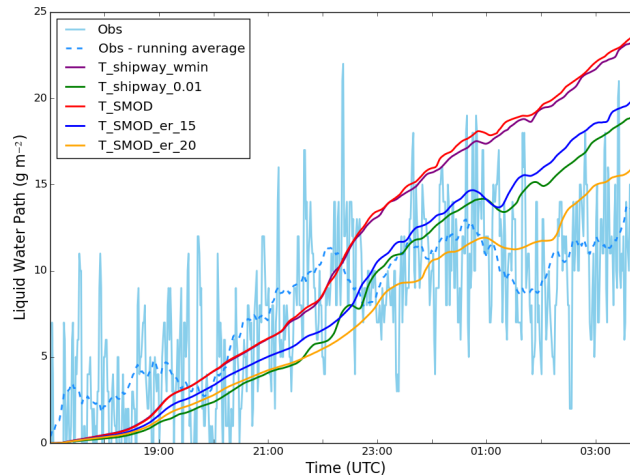


Figure 5. (a) - Time series of the surface deposition rate ($\text{g m}^{-2} \text{hr}^{-1}$). Purple – T_shipway_wmin; green – T_shipway_0.01; red – T_SMOD; blue – T_SMOD_er_15; orange – T_SMOD_er_20; light blue – observations. (b) - Time series of the liquid water path (g m^{-2}). Purple – T_shipway_wmin; green – T_shipway_0.01; red – T_SMOD; blue – T_SMOD_er_15; orange – T_SMOD_er_20; light blue – observations; blue dashed - running average over observations (40 points).

simulated activation and proportion rates lead to the fog layer growing 40 m too deep in comparison to observations. Initially, T_shipway_0.01 has a lowest droplet proportion rate, with the simulated spatial vertical FDNC agreeing best with observations. However, it begins to have activation and proportion rates similar to T_shipway_wmin and T_SMOD. This results suggests that T_shipway_0.01 transition rate to a thicker fog is still too fast, indicating that using an activation scheme driven by just an updraft velocity is unsuitable for fog simulations.

350

Throughout the night, both T_shipway_wmin and T_SMOD have a higher LWP than T_shipway_0.01 (Fig. 5). Poku et al. (2019) showed that the LWP increases with aerosol concentration and hence $\text{CDNC}_{\text{FDNC}}$, with Porson et al. (2011) demonstrating that the increase in $\text{CDNC}_{\text{FDNC}}$ resulted in a stronger downwelling longwave flux, signalling the presence of a deeper fog. T_shipway_wmin has the steepest decrease in the visibility during fog formation, suggesting that it has the highest initial $\text{CDNC}_{\text{FDNC}}$. As these tests all have the same fixed effective radius (unlike studies such as Stolaki et al., 2015),

355

the change in LWP is primarily due to the sedimentation rate, therefore indicating that T_shipway_wmin has the slowest sedimentation rate of all three tests as a result. A decreased sedimentation rate will lead to more liquid water being present in the fog layer. Consequently, this will lead to stronger cooling at the fog top (Poku et al., 2019), strengthening the feedback of increased liquid water production in the layer. This result provides further evidence of how the error in aerosol activation that
360 utilises a w_{min} of 0.1 m s^{-1} impacts the fog, especially during the initial formation stage. The LWP and mean near-surface visibility are not appreciably different between T_shipway_wmin and T_SMOD (Fig. ??b5), suggesting the \overline{CDNC} - \overline{FDNC} is very similar between the two. T_shipway_0.01 has the highest near-surface visibility between 1700 and 2300 UTC by up to 340 m, in addition to the lowest LWP by up to 4 g m^{-2} . Averaged time-height slices of \overline{CDNC} - \overline{FDNC} and LWC were taken for all three tests, showing relatively small changes in the fog layer's \overline{CDNC} - \overline{FDNC} between T_shipway_wmin and T_SMOD
365 (not shown).

So far we have seen that T_SMOD is performing similar to T_shipway_wmin, with T_shipway_0.01 appearing to be the ideal solution for simulating IOPI. However, this may indicate that the default settings for SMOD may not be suitable for our study. The similarity of T_shipway_wmin and T_SMOD suggests that the combined cooling rate in T_SMOD is similar to the cooling rate associated with w_{min} in T_shipway_wmin. To understand whether this is the case, a horizontal slice at $z = 2 \text{ m}$
370 of \overline{CDNC} - \overline{FDNC} and the contributions to the relative cooling rates were taken at different times, as shown in Fig. ??6. As 2 m is not at the model's lowest vertical grid box, there should not be any direct heating from the imposed surface conditions. At 1730 UTC the \overline{CDNC} - \overline{FDNC} is about 83 cm^{-3} (Fig. ??6a), with more than 85% of the total cooling contribution being due to longwave heating (Fig. ??6m). However, later in the night, the cooling contribution to longwave tendencies increases to around 90% within the fog layer (Fig. ??6o), due to a decrease in the adiabatic cooling tendency to about 0.5 K hr^{-1} (Fig.
375 ??6k). Eventually, the fog develops, resulting in the longwave contribution to cooling decreasing to around 15% (Fig. ??6p), with an increase in cooling due to vertical motion. The drop in near-surface longwave cooling occurs as the fog transitions to become optically thick, and so the longwave flux divergence becomes smaller near the surface, while the adiabatic effects become larger due to the onset of convection driven by radiative cooling at the fog top (Mazoyer et al., 2017).

The new SMOD activation scheme is more physically realistic, in that it is coupled to the radiative cooling in the fog, making
380 the scheme potentially more sensitive to the way that this cooling is calculated in the model. Therefore, the assumption of the effective radius being fixed for these simulations may not be suitable to accurately simulate the radiative impact of the fog layer. The following section will present some sensitivity tests to assess the impact of this assumption on fog development.

5.2.1 Sensitivity of SMOD to the effective radius

(a) – Time series of the mean visibility (m) at a 2 m altitude. Purple – T_SMOD; green – T_er_15; red – T_er_20; light blue –
385 observations. The minimum and maximum visibility are marked on the figure by the shaded area. (b) – Time series of the liquid water path (g m^{-2}). Purple – T_SMOD; green – T_er_15; red – T_er_20; light blue – observations; blue dashed – running average over observations (40 points).

Hill et al. (2008) showed the impact of using a fixed effective radius in simulations of stratocumulus clouds on stratocumulus clouds simulations, with studies such as Bierwirth et al. (2013) and Young et al. (2016) showing how the observed effective

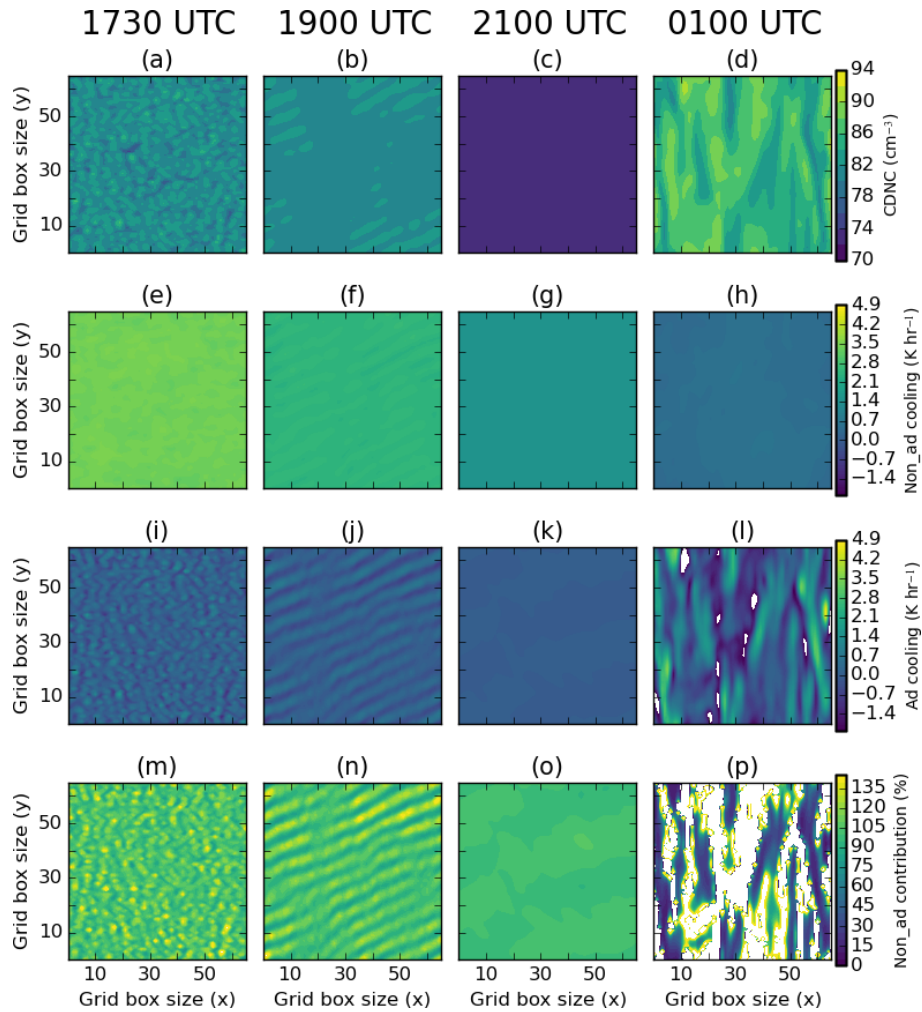


Figure 6. Horizontal slices made at $z = 2$ m of $\overline{CDNC} - \overline{FDNC}$ (cm^{-3}) in T_SMOD at (a) - 1730, (b) - 1900, (c) - 2100 and (d) - 0100 UTC. (e) - (h): non-adiabatic cooling (K hr^{-1}); (i) - (l): adiabatic cooling (K hr^{-1}); (m) - (p): Non-adiabatic cooling contribution (%). Note: for the cooling contribution, white masks out regions where the contribution is greater than 140 (%).

390 radius in arctic clouds can change (between 5 to 15 μm) in relation to the cloud's LWC and $\overline{CDNC} - \overline{FDNC}$. As this variability may be key to modelling radiation fog using the SMOD activation scheme, two tests were conducted that investigated the fog's sensitivity to a change in r_e .

When increasing r_e from 10 to 20 μm , the near-surface visibility increases by up to 40%, and decreases the LWP by up to 42% (Fig. ??). ~~However, whilst~~ 3a). Furthermore, increasing r_e leads to the simulated SHF better agreeing with observations, despite it still being positive later in the night (Fig. 3b). ~~However, although~~ increasing r_e results in the LWP agreeing better with observations (Fig. 5), neither test captures the changes in near-surface visibility during fog formation. ~~Bergot et al. (2015) showed that~~ (Fig. 3b). Previous studies (e.g. Bergot et al., 2015; Ducongé et al., 2020) argued that it's critical to account for a

395

heterogeneous terrain when simulating the fog's ~~spatial variability during initial formation had been impacted when their simulations included a heterogeneous terrain~~ initial spatial variability. However, Cardington is relatively homogeneous and hence potentially highlights a further discrepancy in the aerosol representation in these simulations. As an example, in-cloud removal (nucleation scavenging) has not been accounted for in this work, which has been shown to impact the spatial variability and development of mixed-phased clouds (Miltenberger et al., 2018). In addition, the discrepancy in our results may be due to these simulations utilising a bulk microphysics scheme, which has been shown to not account for hydrated and small newly formed droplets (Schwenkel and Maronga, 2020). Nonetheless, the decrease in liquid water indicates that the fog's development in optical thickness has slowed down with an increase in r_e and hence the importance of coupling both CASIM and SOCRATES together. Going forward, future studies should use a coupled r_e as this should, in theory, lead to an improvement in ~~CDNC~~ FDNC as the better representation in aerosol activation in the SMOD scheme will feed into the radiation scheme.

Figure ??-7 shows time-height slices of ~~CDNC~~ FDNC and LWC for T_SMOD, T_SMOD_er_15 and T_SMOD_er_20. Before 2145 UTC, the ~~CDNC~~ FDNC in T_SMOD is strongest towards the top at around 80 cm^{-3} . After this time, it increases throughout the fog layer to a range between 86 and 94 cm^{-3} (Fig. ??7a). These changes in FDNC can be noted when compared to observations, where both T_SMOD_er_15 and T_SMOD_er_20 begins to have a less uniform structure throughout the fog layer (Fig. 4). Coinciding with this is an increase in LWC from 0.2 to 0.24 g kg^{-1} , suggesting the time at which the fog began to develop and grow in optical thickness. However, an increase in r_e results in delayed onset of the growth in optical thickness to 2300 and 0030 UTC for T_SMOD_er_15 and T_SMOD_er_20 respectively. The ~~CDNC~~ FDNC on average decreases for both T_SMOD_er_15 and T_SMOD_er_20 across the whole fog layer, with a noticeable rise at around 2300 UTC for T_SMOD_er_15. Although this pattern is the same for T_SMOD_er_20, there are periods where there are visible decreases in ~~CDNC~~ FDNC, e.g. between 0130 and 0230 UTC (Figs. ??7c and e respectively). A combination of both the ~~CDNC~~ FDNC and LWC decreasing results in a slower transition in the fog layer, which is shown in the downwelling longwave at 2 m (Fig. ??8). The downwelling longwave decreases by a maximum of 20 W m^{-2} between T_SMOD and T_SMOD_er_20, with T_SMOD_er_20 undergoing the slowest ~~rate of increase~~ positive rate with all the simulations presented in this paper. There are differences between the observed and simulated downwelling in all three simulations, however, before 2200 UTC, T_SMOD_er_20 decreases this difference to a maximum of 10 W m^{-2} .

SOCRATES calculates the longwave radiative fluxes by the cloud's optical depth, τ , (Edwards and Slingo, 1996):

$$\tau = k^{(e)} \Delta m, \quad (13)$$

such that Δm is the change in mass for a given spectral band and $k^{(e)}$ is the mass extinction coefficient, which is defined as:

$$k^{(e)} = L \left(a + \frac{b}{r_e} \right). \quad (14)$$

For SMOD scheme, both the ~~CDNC~~ FDNC and LWC is sensitive to r_e , given Eq's (13) and (14). This leads to a more physical representation of aerosol activation that should be considered when simulating cases of fog. These results demonstrate the importance of an accurate effective radius and the reasons for using a coupled r_e , given its impact on the fog evolution.

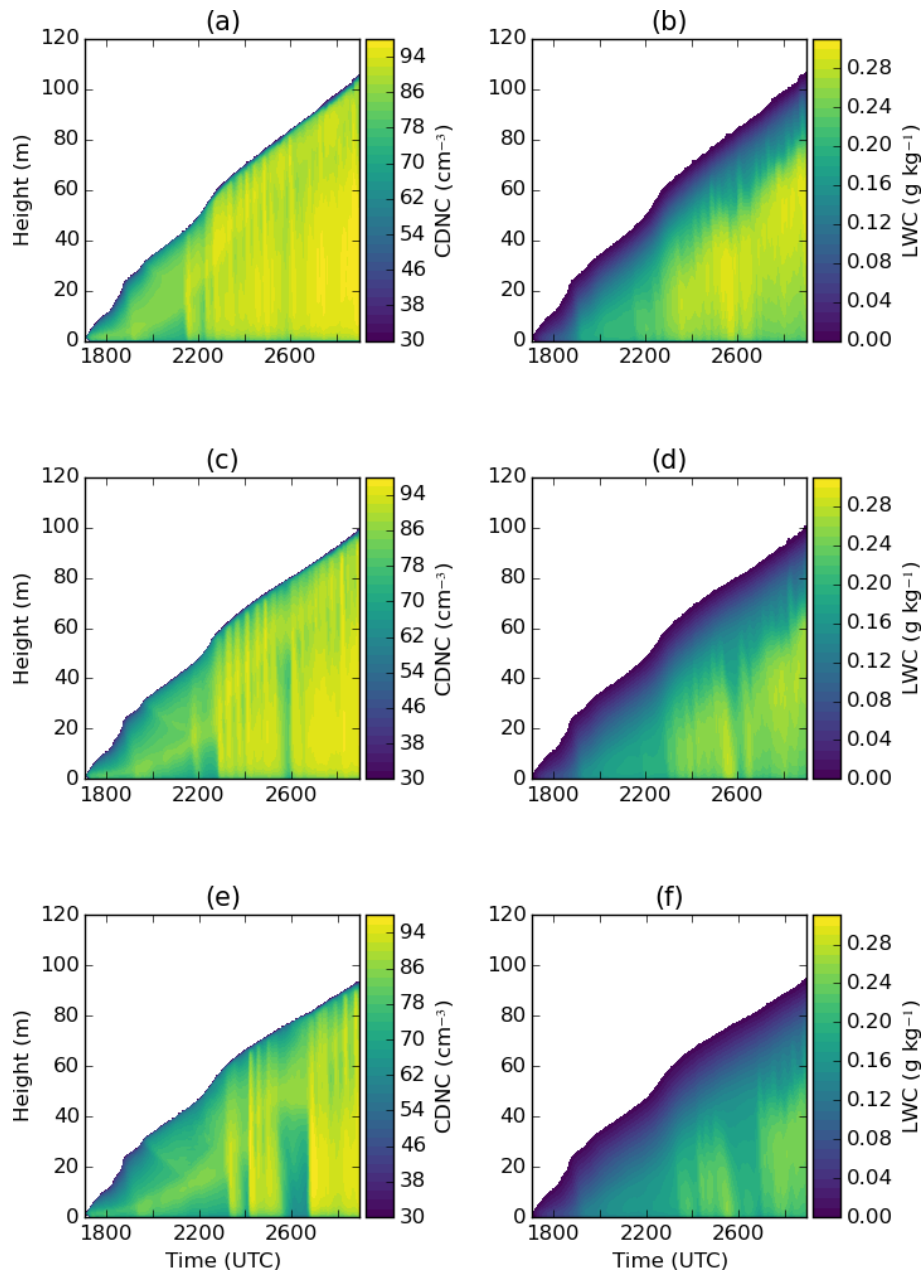


Figure 7. Plots of (a), (c), (e) - mean $\overline{\text{CDNC}}_{\text{FDNC}}$ (cm^{-3}); and (b), (d), (f) - mean LWC (g kg^{-1}). (a), (b): T_SMOD; (c), (d): T_SMOD_er_15; (e), (f): T_SMOD_er_20.

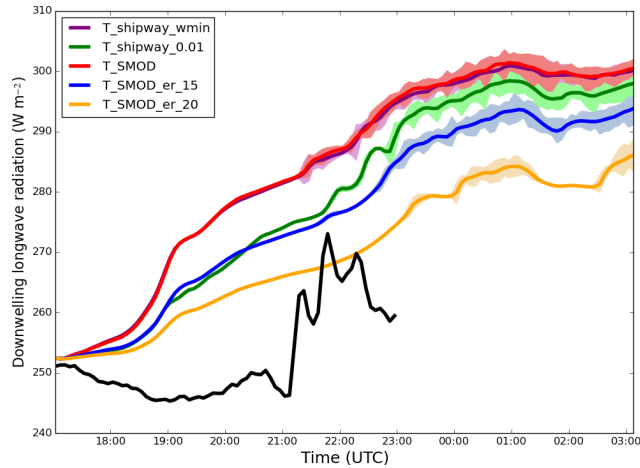


Figure 8. Time series of the downwelling longwave radiation (W m^{-2}) at a 2 m altitude. Purple – $T_{\text{shipway_wmin}}$; green – $T_{\text{shipway_0.01}}$; red – T_{SMOD} ; blue – $T_{\text{SMOD_er_15}}$; red-orange – $T_{\text{SMOD_er_20}}$; black – observations. The minimum and maximum downwelling longwave radiation are marked on the figure by the shaded area.

430 6 Discussion

This work aimed to investigate how the representation of aerosol activation influenced **simulations of** nocturnal radiation fog **simulations**. There was a strong focus on critiquing the assumptions used in several current aerosol activation schemes, which are usually designed for clouds where cooling is driven by adiabatic ascent. This work addressed two research questions.

6.1 What are the potential differences in aerosol activation between the Shipway and SMOD scheme?

435 The assumptions used in the Shipway (2015) scheme to date, i.e. the use of just an updraft velocity with a minimum threshold w_{min} , were tested against the SMOD scheme in an offline box model. The sensitivity of Shipway to w_{min} was first tested. For accumulation and coarse mode aerosol, there was a monotonical decrease in $N_{act} - N_{act}$ as w_{min} approached 0 m s^{-1} . These tests also highlighted the stepwise function present in Aitken mode aerosol in the low updraft velocity regime. Given
 440 activation in fog based on the range of environmental aerosol size distributions, as the required environmental supersaturation for impact is substantially higher than supersaturation's seen in reality. However, the stepwise behaviour was caused by the poor resolution in the look-up table that calculated $s_{max} - s_{max}$ in this regime, therefore demonstrating why just removing w_{min} with no alternative cooling source may not be an appropriate solution when simulating aerosol activation in fog.

For accumulation mode aerosol, there were noticeable percentage differences between the actual cooling rate and the use of a
 445 w_{min} equal to 0.1 m s^{-1} (as typically used in clouds) by up to 70%, as the environment becomes more polluted. In reality, for a given liquid water path, increasing the aerosol concentration will result in a larger concentration of smaller droplets, increasing the fog's optical depth (Twomey, 1977), and may cause the fog to become well-mixed too quickly. Therefore for this example,

a similar effect could occur should an unsuitable w_{min} be used in fog simulations. In addition, these tests demonstrated that using an aerosol activation scheme that assumes just adiabatic ascent may potentially underestimate N_{act} by 20% in an environment driven by non-adiabatic cooling processes (i.e. fog formation). Furthermore, the associated percentage difference in the choice of w_{min} would be the same should SMOD be run with just an adiabatic cooling source, given there were no differences in $C_{adiabatic}$ -Shipway and SMOD in an adiabatic setup. Consequently, both of these results show that the aerosol indirect effects may not be properly accounted for in simulations of fog fog simulations when using a traditional aerosol activation scheme.

455 6.2 How do the differences in aerosol activation representation impact on the fog evolution in a large eddy simulation?

The Shipway (2015) aerosol activation scheme was used to test the impact w_{min} could have on simulating fog in MONC using only accumulation mode aerosol. It was shown that a reduction in w_{min} lowered the initial $CDNC$ - $FDNC$ during formation, resulting in the fog undergoing a slower transition to a well-mixed layer. Reducing w_{min} to 0.01 m s^{-1} displayed some unusual model behaviours during fog formation, which is most likely driven by the model's spin-up period, rather than shear or convection motion. However, the only way to confirm this is to initialise the model earlier, which is not possible with the given radiosonde data from IOP1. Upon initial analysis, there was not an improved performance using the SMOD scheme against the Shipway scheme with an applied w_{min} of 0.1 m s^{-1} . However Upon further inspection, it was shown that the cause of this result was due to r_e not reflecting the change in $CDNC$ - $FDNC$. When r_e was increased from 10 to $20 \mu\text{m}$, the result was a slower transition to a well-mixed layer, which was more in line with observations of IOP1. This highlighted the importance of the effective radius and provides further motivation to couple the effective radius with a change in $CDNC$ - $FDNC$. However, despite this result using the SMOD scheme, our work has highlighted potential physical processes regarding aerosol missing in this study, demonstrating the complexities when simulating aerosol-fog interactions in nocturnal radiation fog.

7 Conclusions

470 This work has demonstrated the unsuitability of using an aerosol activation scheme designed for convective clouds in fog simulations. This complements, complementing previous studies such as Schwenkel and Maronga (2019), who have shown how the choice in aerosol activation scheme impacts the fog evolution through a change in the $CDNC$. However, by designing a scheme that is also dependent on $FDNC$. Similar to our study, they and authors such as Mazoyer et al. (2017) have used a similar mathematical framework with their choice in using a non-adiabatic cooling source, the results in this paper have demonstrated the importance of aerosol activation representation when trying to accurately capture the fog's transition to a well-mixed layer. Previous studies (e.g. Mazoyer et al., 2017) have investigated the fog evolution while accounting for a radiative cooling tendency in the change in supersaturation. However in aerosol activation scheme first utilised by Zhang et al. (2014). Our work in this paper compliments this and other studies by doing the following:

480 1. Although as suggested by Boutle et al. (2018) that the solution is to remove the w_{min} threshold when simulating radiation fog, our results show that this is not necessarily a suitable option. This is highlighted with T_shipway_0.01, which although did initially perform better than the rest of the tests discussed, it transitioned to a thicker fog than both T_SMOD_er_15 and T_SMOD_er_20. As aerosol activation in T_shipway_0.01 was driven by just an updraft velocity, this suggests why a more physical based activation scheme such as SMOD is critical to simulate nocturnal radiation fog. More specifically, the choice in activation scheme is key when the fog layer may transition to an optically thick layer.

485 2. Although there has been studies investigating the use of the non-adiabatic framework in fog simulations, this is the first study ~~that has investigated the change in cooling due to non-adiabatic processes in~~ to the author's knowledge that critiques this framework with a fog case that formed in a clean aerosol ~~regime, making it beneficial in aiding the understanding the impact~~ regimes (accumulation $CCN < 100 \text{ cm}^{-3}$ as defined by Boutle et al., 2018), therefore supporting previous ~~literature on the topic~~ of aerosol-fog interactions ~~during nocturnal radiation fog~~.

490 Work to develop the SMOD scheme is still ongoing and will include ~~accounting a total non-adiabatic cooling tendency that will account~~ for additional non-adiabatic processes such as turbulent or subgrid mixing. Completing this work could make it easier to incorporate the SMOD scheme into a model such as an NWP model. This is because the non-adiabatic process would be a change in temperature within the grid box, rather than requiring an explicit additional term. It was shown that SMOD is sensitive to SOCRATES with regards to the fixed effective radius, especially when considering the decrease in ~~CDNC~~FDNC.

495 Therefore, future work should run the new scheme with the interactive coupling of r_e to CASIM, should the option be available.

As noted in Section 5.2, SMOD was unable to capture the fog's spatial variability during initial formation. ~~However,~~ Poku et al. (2019) discussed how using a more "realistic" activation scheme such as SMOD would be a suitable solution, as the FDNC would be able to capture the fog's transitional period. However, although our work has shown that SMOD may be a better option than Shipway, none of our simulations were able simulate both the initial fog formation variability

500 and remain stable throughout the night. This feature may have been due to our study using a bulk microphysics scheme, and more specifically a saturation adjustment condensation calculation, which has shown to be problematic in other cloud regimes (e.g. surface precipitation in convective clouds Lebo et al., 2012). Previous LES studies of IOP1 (e.g. Boutle et al., 2018) have addressed this limitation by using a prognostic for supersaturation, which in their works led to a reasonable transition to when the fog became optically thick. In addition, Schwenkel and Maronga (2020) proposed moving away from bulk microphysics

505 schemes and instead uses a lagrangian cloud model (LCM), which can account for small droplets and swollen aerosols (for context, our results do not capture changes in the drop-size distribution with aerosol activation representation). Therefore, future work should include simulating IOP1 using a LCM, which could be capable to improve capturing the features of a thin fog. However, as our study was motivated to develop and test a suitable scheme that could be used in NWP to account for aerosol impacts in fog, a LCM mechanism may be unsuitable in an NWP due to additional computational expense. Furthermore, using

510 a prognostic for supersaturation is unsuitable due to the timestep for changes in supersaturation being too small for most NWP (Morrison and Gettelman, 2008). Miltenberger et al. (2018) showed that by including in-cloud aerosol removal, the source of aerosol began depleting through nucleation, resulting in a more open-cell cloud structure and changes in the cloud dynamics.

As this study was done using a bulk microphysics scheme, this may be a suitable option when testing the SMOD scheme. To date, there are no studies that have investigated the use of a nucleation scavenging parameterisation in fog in the context of bulk microphysical parameterisations, therefore suggesting a future piece of work within the subject of aerosol-fog interactions. For this work, there was a lack of simultaneous measurements of observed aerosol and cloud droplets. Given the w_{min} 's sensitivity to aerosol concentration, having these measurements in future studies will both help constrain the model and highlight any further discrepancies in aerosol activation representation in fog. Finally, our study has focused on the first 10 hours of IOP1 and hence has not accounted for the fog evolution during daytime. Given the impact additional processes such as aerosol-radiation interactions and interactive surface scheme will have on fog dissipation, it's critical to ensure schemes such as SOCRATES and CASIM are coupled for this future work.

As a wider implication, aerosol-cloud interactions are a big source of uncertainty when modelling atmospheric processes, both within forecasting (NWP) and climate (GCM) models and the choice of aerosol activation can influence how big this uncertainty is. Typically, the resolution of NWP and GCM model simulations is very coarse compared to LES, meaning that any present updraft velocities are usually subgrid and hence cannot be resolved. To represent aerosol activation on a subgrid level, the vertical velocity is either in the form a characteristic vertical velocity (e.g. Ghan et al., 1997) or a PDF function based on the vertical velocity (e.g. West et al., 2014). More recently, Malavelle et al. (2014), for example, discussed methods to account for subgrid velocities used in aerosol activation in convection-permitting models. These methods utilise a w_{min} , however, this should be lowered systematically for future work regarding aerosol activation in fog. Although gaining measurements of vertical velocity PDFs could be difficult in fog, the results presented in this paper could provide a useful framework to estimate what the variation in vertical velocities in fog could be, therefore providing a good estimation of the types of distributions that best match these velocities. Finally, to have a full cooling term applied in an NWP model, it is important to know how these vertical velocities correlate with the changes in non-adiabatic cooling.

This paper has shown the need to differentiate between optically thin fog ($w_{min} \approx 0 \text{ m s}^{-1}$) and optically thick fog, where sub-grid vertical velocities can be important. The method being presented in this work is computationally efficient and provided an additional level of flexibility consider different cooling sources in cases where updrafts are not the dominant cooling source. Given this flexibility, this will allow the SMOD scheme to undergo further testing in both high resolution and NWP models. Whilst this has been tested in only the Shipway and SMOD activation schemes, the framework for a change in supersaturation is generic enough for it to be applied to other activation schemes too.

540 **Appendix A: Mathematical formulation for the change in supersaturation**

Pruppacher and Klett (2010) defined supersaturation in terms of the water vapour mixing ratio, q_v , as:

$$q_v = (1 + s) \left(\frac{\epsilon e_s}{p} \right), \quad (\text{A1})$$

where p is the pressure of dry air, s is the environment's supersaturation, e_s is the saturation vapour pressure and $\epsilon = \frac{R_a}{R_v} = 0.622$; the ratio of the gas constant of dry air to water vapour. Differentiating Eq. (A1) with respect to time, and rearranging for
 545 the change in supersaturation gives:

$$\frac{ds}{dt} = \left(\frac{p}{\epsilon e_s} \right) \frac{dq_v}{dt} - (1+s) \left[\frac{1}{e_s} \frac{de_s}{dt} - \frac{1}{p} \frac{dp}{dt} \right]. \quad (\text{A2})$$

The Clausius-Clapeyron equation is defined as:

$$\frac{de_s}{dT} = \frac{Le_s}{R_v T^2}, \quad (\text{A3})$$

with L being defined as specific latent heat. Applying the chain rule gives:

$$\begin{aligned} \frac{de_s}{dt} &= \frac{Le_s}{R_v T^2} \left. \frac{dT}{dt} \right|_{tot} \\ 550 \quad &= \frac{Le_s}{R_v T^2} \left[\left. \frac{dT}{dt} \right|_{ad} + \left. \frac{dT}{dt} \right|_{non_ad} + \left. \frac{dT}{dt} \right|_{lat} \right]. \end{aligned} \quad (\text{A4})$$

$\left. \frac{dT}{dt} \right|_{ad}$ is the change in temperature due to dry adiabatic processes, such that:

$$\left. \frac{dT}{dt} \right|_{ad} \equiv -\Gamma \frac{dz}{dt} = -\Gamma w; \quad (\text{A5})$$

where $\Gamma = \frac{g}{c_p}$, the dry adiabatic lapse rate with c_p being the specific heat capacity, and w is the updraft velocity. $\left. \frac{dT}{dt} \right|_{non_ad}$
 555 is the change in temperature due to non-adiabatic processes (e.g. radiative cooling, turbulent mixing), that excludes latent heat release, and $\left. \frac{dT}{dt} \right|_{lat}$ is the change in temperature due to latent heat release i.e. condensation/evaporation. For adiabatic expansion (lifting), there are corresponding pressure and temperature changes (that satisfy the first law of thermodynamics). However, for isobaric non-adiabatic heating processes, there is no change in p but there is a change in T that modifies Eq. (A4). Therefore, for the change in p , by:

1. assuming hydrostatic equilibrium, where $\frac{dp}{dz} = -\rho g$;
- 560 2. using the equation for the ideal gas law, where $p = \rho R_a T$;

$$\begin{aligned} \frac{dp}{dt} &= \frac{dp}{dz} \frac{dz}{dt} \\ &= -\frac{pg}{R_a T} w. \end{aligned} \quad (\text{A6})$$

The change in temperature due to latent heat release is proportional to the change in vapour mixing ratio, such that:

$$\left. \frac{dT}{dt} \right|_{lat} = -\frac{L}{c_p} \left. \frac{dq_v}{dt} \right|_{cond} = \frac{L}{c_p} \frac{dq_l}{dt}. \quad (\text{A7})$$

Inserting Eq.'s (A4), (A6) and (A7) into Eq. (A2), and assuming $1 + s \approx 1$ gives:

$$565 \quad \frac{ds}{dt} = \left(\frac{Lg}{R_v T^2 c_p} - \frac{g}{R_a T} \right) w - \frac{L}{R_v T^2} \left. \frac{dT}{dt} \right|_{non_ad} - \left(\frac{p}{\epsilon \epsilon_s} + \frac{L^2}{R_v c_p T^2} \right) \frac{dq_l}{dt}. \quad (\text{A8})$$

Eq. (A8) can be used to simulate aerosol activation in both fog and convective cloud regimes, highlighting the flexibility of the SMOD scheme. As an objective for this work is to understand how using an adiabatic framework to represent aerosol activation in a non-adiabatic environment (e.g. fog) may impact N_{act} , w in Eq.(A8) will be rewritten as $\left. \frac{dT}{dt} \right|_{ad}$, such that:

$$\frac{ds}{dt} = \psi_1 \left. \frac{dT}{dt} \right|_{ad} + \psi_2 \left. \frac{dT}{dt} \right|_{non_ad} - \gamma \frac{dq_l}{dt}, \quad (\text{A9})$$

570 where:

$$\psi_1 = \frac{c_p}{R_a T} - \frac{L}{R_v T^2},$$

$$\psi_2 = -\frac{L}{R_v T^2}, \quad (\text{A10})$$

$$\gamma = \frac{p}{\epsilon \epsilon_s} + \frac{L^2}{R_v c_p T^2}.$$

Appendix B: Fitting modelled LWP and cloud drop-size distribution to observations - shape parameter

All tests in this paper assume a fixed r_e , implying that the change in liquid water is controlled by the sedimentation rate, as discussed in Poku et al. (2019). The sedimentation rate is controlled by the cloud drop-size distribution (see Eq. 11), with its skewness being determined by the shape parameter, μ_d . Mazoyer et al. (2017) adapted the default shape parameter to best fit the modelled cloud drop-size distribution to observations. For this work, a similar approach would have ideally been chosen to find a suitable μ_d to capture the changes in liquid water. However, the instrumentation only began to record spectra during IOP1 4 hours into the observed fog case, and by this time, the layer had already begun to grow in optical thickness. To account for this limitation, the LWP was used to decide on a suitable choice of μ_d . These simulations were then compared to the available IOP1 cloud spectra data, to validate and hence choose a μ_d going forward. For this fitting, μ_d ranged from 0 to 3, with these tests denoted as T_mu_0, T_mu_1, T_mu_2 and T_mu_3 respectively. Although simulations were conducted to increase the shape parameter up to a value of $\mu_d = 7$ (similar to Mazoyer et al., 2017), the LWP for tests where $\mu_d > 4$ were higher than the observed mean LWP and hence these results will not be shown.

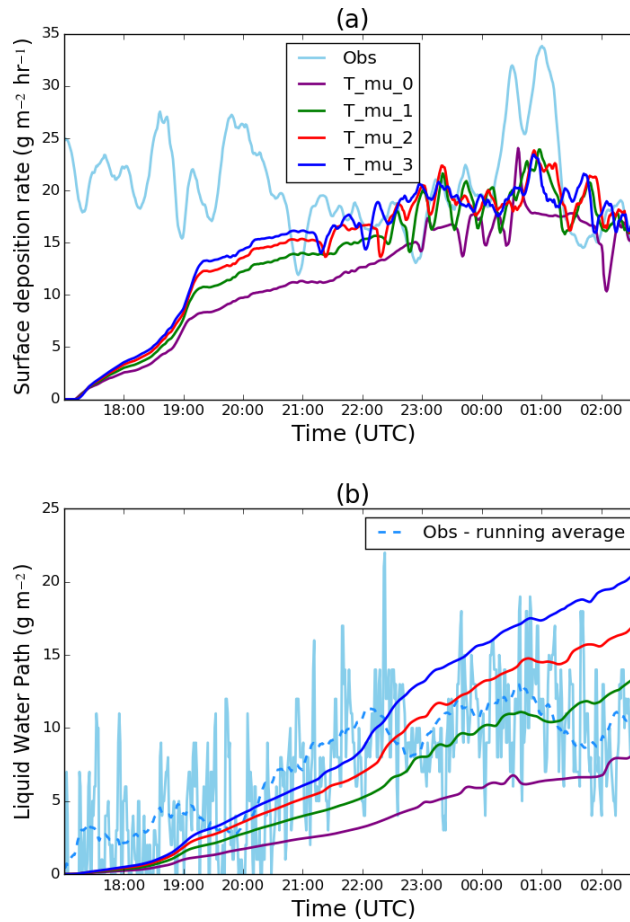


Figure B1. a) - Time series of the surface deposition rate ($\text{g m}^{-2} \text{hr}^{-1}$). Purple – T_mu_0; green – T_mu_0; red – T_mu_1; dark blue – T_mu_3; light blue – observations. (b) Time series of the liquid water path (g m^{-2}). Purple – T_control; green – T_mu_1; red – T_mu_2; dark blue – T_mu_3; light blue – observations; blue dashed – running average over observations (40 points).

Both the surface deposition rate and LWP increase with μ_d (Figs. [??B1a-b](#)), with this increase being more inline with observations. T_mu_2 and T_mu_3 both show improved LWP when compared to observations, especially before 2200 UTC. As there are potentially multiple options in choosing μ_d , the modelled cloud drop-size distribution was compared to observations, as shown in Fig. [??B2](#). Prior to 2200 UTC, all shape parameter tests began with an abundance of small droplets, signalling the formation of fog, and the density of small droplets being greatest in T_mu_0 (not shown). During fog evolution, all tests begin moving right in terms of skewness with the exception for T_mu_0 (due to T_mu_0 being logarithmic). For the tests where $\mu_d > 0$, increasing the shape parameter results in the peak of the distribution decreasing and moving to the right, for all tested time frames. For example, increasing the shape parameter to $\mu_d = 3$ results in a peak droplet diameter of $11 \mu\text{m}$. These results suggest a limitation in the default choice in $\mu_d = 0$ and hence the assumption of a logarithmic distribution for fog development

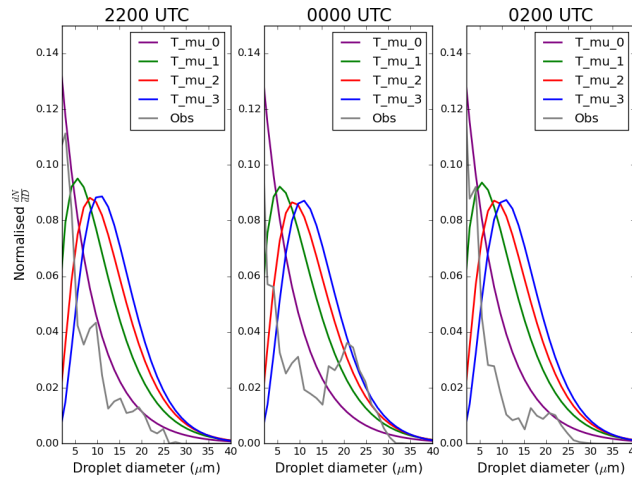


Figure B2. Cloud drop-size distributions for shape parameter simulations at 1710, 1800 and 2200 UTC at 2 m. T_mu_0; green – T_mu_0; red – T_mu_1; dark blue – T_mu_3; grey - observations.

during IOP1. By increasing the shape parameter during the fog evolution, fewer large droplets will sediment out of the fog layer, therefore explaining the presence of bigger droplets still within the system in these tests (for example, tests T_mu_1 - 3).

595 At 2200 UTC, the observed cloud droplet spectrum mostly follows a logarithmic distribution, however, later in the night, it evolves more into a bi-modal distribution (as seen in Price, 2011). For example, at 0000 UTC, the peaks occur at 8 and 22 μm . Of the shape parameter tests, the observations are in best agreement with T_mu_3 for droplet size diameters between 22 to 27 μm at 0000 UTC, however, this fit does not take into account the peak shown within the smaller droplets. In an ideal situation, a modelled cloud drop-size distribution would take into account the bi-modal nature shown within the distribution. In reality, it
 600 is likely that these smaller droplets have not activated, but instead are a source of hydrated aerosol which can contribute up to 68% of the total light scattered, and hence result in the reduction in visibility within the fog (Hammer et al., 2014). However, although these smaller droplets may potentially change the microphysical structure of the fog, the introduction of a bi-modal distribution (or a varying shape parameter) within CASIM may increase model computational expense, with no appreciable changes in the fog evolution. Given these results, a shape parameter of $\mu_d = 3$ will be used in this paper.

605 *Author contributions.* CP undertook the research, carried out the simulations and analysis, and led the writing of the paper. AR, AB, AH contributed to the research design, interpretation of the results and the writing of the final paper. AH provided technical support with MONC. BS provided the box model and supported its use.

Code availability. The MONC, CASIM, offline box model and SOCRATES codes are maintained by the Met Office and accessible via the Met Office Science Repository Service (<https://code.metoffice.gov.uk/>) (last access: 1st March 20210). The MONC branch is available at

610 https://code.metoffice.gov.uk/svn/monc/main/branches/dev/craigpoku/r6496_MONC_poku_activation (last access: 28th August 2020). The CASIM branch is available at https://code.metoffice.gov.uk/svn/monc/casim/branches/dev/craigpoku/vn0.3.2_poku_scheme_debugged (last access: 1st March 2021). The offline box model branch is available at https://code.metoffice.gov.uk/svn/monc/casim/branches/dev/craigpoku/r287_Offline_Activation (last access: 1st March 2021). For further details, please contact Adrian Hill (adrian.hill@metoffice.gov.uk)

Competing interests. The authors declare that there are no competing interests.

615 *Acknowledgements.* The authors would like to thank the Met Office Research Unit in Cardington (UK) for providing and processing the observational dataset used throughout this study. CP was supported by a Natural Environment Research Council (NERC) Industrial CASE award with the Met Office (grant number NE/M009955/1). This work used Monsoon2, a collaborative High Performance Computing facility funded by the Met Office and the Natural Environment Research Council. [The authors would like to thank the anonymous reviewers for comments that helped improve the quality of this manuscript.](#)

620 References

- Abdul-Razzak, H. and Ghan, S. J.: A parameterization of aerosol activation: 2. Multiple aerosol types, *Journal of Geophysical Research: Atmospheres*, 105, 6837–6844, <https://doi.org/10.1029/1999JD901161>, <http://doi.wiley.com/10.1029/97JD03735>, 2000.
- Abdul-Razzak, H., Ghan, S. J., and Rivera-Carpio, C.: A parameterization of aerosol activation: 1. Single aerosol type, *Journal of Geophysical Research: Atmospheres*, 103, 6123–6131, <https://doi.org/10.1029/97JD03735>, 1998.
- 625 Abramowitz, M. and Stegun, I. A.: *Handbook of mathematical functions*, Courier Corporation, <http://people.math.sfu.ca/~cbm/aands/intro.htm>, 1965.
- Albrecht, B. A.: Aerosols, cloud microphysics, and fractional cloudiness., *Science*, 245, 1227–1230, <https://doi.org/10.1126/science.245.4923.1227>, <http://www.ncbi.nlm.nih.gov/pubmed/17747885>, 1989.
- BBC: Sheppey crossing crash: Dozens hurt as 130 vehicles crash - BBC News, <https://www.bbc.co.uk/news/uk-england-kent-23970047>,
630 2013.
- Bergot, T., Escobar, J., and Masson, V.: Effect of small-scale surface heterogeneities and buildings on radiation fog: Large-eddy simulation study at Paris-Charles de Gaulle airport, *Quarterly Journal of the Royal Meteorological Society*, 141, 285–298, <https://doi.org/10.1002/qj.2358>, <http://doi.wiley.com/10.1002/qj.2358>, 2015.
- Bierwirth, E., Ehrlich, A., Wendisch, M., Gayet, J.-F., Gourbeyre, C., Dupuy, R., Herber, A., Neuber, R., and Lampert, A.: Climate of the
635 Past Geoscientific Instrumentation Methods and Data Systems Optical thickness and effective radius of Arctic boundary-layer clouds retrieved from airborne nadir and imaging spectrometry, *Atmos. Meas. Tech*, 6, 1189–1200, <https://doi.org/10.5194/amt-6-1189-2013>, www.atmos-meas-tech.net/6/1189/2013/, 2013.
- Böing, S. J., Dritschel, D. G., Parker, D. J., and Blyth, A. M.: Comparison of the Moist Parcel-in-Cell (MPIC) model with large-eddy simulation for an idealized cloud, *Quarterly Journal of the Royal Meteorological Society*, 145, 1868–1881, <https://doi.org/10.1002/qj.3532>,
640 <https://onlinelibrary.wiley.com/doi/abs/10.1002/qj.3532>, 2019.
- Bott, A.: On the influence of the physico-chemical properties of aerosols on the life cycle of radiation fogs, *Boundary-Layer Meteorology*, 56, 1–31, <https://doi.org/10.1007/BF00119960>, <http://link.springer.com/10.1007/BF00119960>, 1991.
- Boutle, I., Price, J., Kokkola, H., Romakkaniemi, S., Kudzotsa, I., Kokkola, H., and Romakkaniemi, S.: Aerosol-fog interaction and the transition to well-mixed radiation fog, *Atmos. Chem. Phys*, 18, 7827–7840, <https://doi.org/10.5194/acp-18-7827-2018>, <https://www.atmos-chem-phys-discuss.net/acp-2017-765/acp-2017-765.pdf><https://doi.org/10.5194/acp-18-7827-2018>, 2018.
645
- Brown, N., Weiland, M., Hill, A., Shipway, B., Maynard, C., Allen, T., and Rezny, M.: A Highly Scalable Met Office NERC Cloud Model, in: *Proceedings of the 3rd International Conference on Exascale Applications and Software*, p. 137, University of Edinburgh, <https://dl.acm.org/citation.cfm?id=2820083.2820108>, 2015.
- Brown, N., Weiland, M., Hill, A., and Shipway, B.: In situ data analytics for highly scalable cloud modelling on Cray machines, *Concurrency and Computation: Practice and Experience*, 30, e4331, <https://doi.org/10.1002/cpe.4331>, <http://doi.wiley.com/10.1002/cpe.4331>, 2018.
650
- Cohard, J.-M., Pinty, J.-P., and Bedos, C.: Extending Twomey’s Analytical Estimate of Nucleated Cloud Droplet Concentrations from CCN Spectra, *Journal of the Atmospheric Sciences*, 55, 3348–3357, [https://doi.org/10.1175/1520-0469\(1998\)055<3348:ETSABO>2.0.CO;2](https://doi.org/10.1175/1520-0469(1998)055<3348:ETSABO>2.0.CO;2), <http://journals.ametsoc.org/doi/abs/10.1175/1520-0469%281998%29055%3C3348%3AETSABO%3E2.0.CO%3B2>, 1998.
- Dearden, C., Hill, A., Coe, H., and Choulaton, T.: The role of droplet sedimentation in the evolution of low-level clouds over southern West
655 Africa, *Atmos. Chem. Phys*, 18, 14 253–14 269, <https://doi.org/10.5194/acp-18-14253-2018>, <https://doi.org/10.5194/acp-18-14253-2018>, 2018.

- Ducongé, L., Lac, C., Vié, B., Bergot, T., and Price, J. D.: Fog in heterogeneous environments: the relative importance of local and non-local processes on radiative-advective fog formation, *Quarterly Journal of the Royal Meteorological Society*, 146, 2522–2546, <https://doi.org/10.1002/qj.3783>, <https://onlinelibrary.wiley.com/doi/10.1002/qj.3783>, 2020.
- 660 Edwards, J. M. and Slingo, A.: Studies with a flexible new radiation code. I: Choosing a configuration for a large-scale model, *Quarterly Journal of the Royal Meteorological Society*, 122, 689–719, <https://doi.org/10.1002/qj.49712253107>, <http://doi.wiley.com/10.1002/qj.49712253107>, 1996.
- Gerber, H.: Supersaturation and Droplet Spectral Evolution in Fog, *Journal of the Atmospheric Sciences*, 48, 2569–2588, [https://doi.org/10.1175/1520-0469\(1991\)048<2569:SADSEI>2.0.CO;2](https://doi.org/10.1175/1520-0469(1991)048<2569:SADSEI>2.0.CO;2), <http://journals.ametsoc.org/doi/abs/10.1175/1520-0469%281991%29048%3C2569%3ASADSEI%3E2.0.CO%3B2>, 1991.
- 665 Ghan, S. J., Chung, C. C., and Penner, J. E.: A parameterization of cloud droplet nucleation part I: single aerosol type, *Atmospheric Research*, 30, 198–221, [https://doi.org/10.1016/0169-8095\(93\)90024-I](https://doi.org/10.1016/0169-8095(93)90024-I), <https://www.sciencedirect.com/science/article/pii/016980959390024I>, 1993.
- Ghan, S. J., Leung, L. R., Easter, R. C., and Abdul-Razzak, H.: Prediction of cloud droplet number in a general circulation model, *Journal of Geophysical Research: Atmospheres*, 102, 21 777–21 794, <https://doi.org/10.1029/97JD01810>, <http://doi.wiley.com/10.1029/97JD01810>, 1997.
- 670 Gray, M. E. B., Petch, J., Derbyshire, S. H., Brown, A. R., Lock, A. P., Swann, H. A., and Brown, P. R. A.: Version 2.3 of the Met. Office large eddy model, *Met Office (APR) Turbulence and Diffusion Rep*, 276, 2001.
- Grosvenor, D. P., Field, P. R., Hill, A. A., and Shipway, B. J.: The relative importance of macrophysical and cloud albedo changes for aerosol-induced radiative effects in closed-cell stratocumulus: insight from the modelling of a case study, *Atmospheric Chemistry and Physics*, 17, 5155–5183, <https://doi.org/10.5194/acp-17-5155-2017>, <https://www.atmos-chem-phys.net/17/5155/2017/>, 2017.
- 675 Gultepe, I., Müller, M. D., Boybeyi, Z., Gultepe, I., Müller, M. D., and Boybeyi, Z.: A New Visibility Parameterization for Warm-Fog Applications in Numerical Weather Prediction Models, *Journal of Applied Meteorology and Climatology*, 45, 1469–1480, <https://doi.org/10.1175/JAM2423.1>, <http://journals.ametsoc.org/doi/abs/10.1175/JAM2423.1>, 2006.
- 680 Gultepe, I., Tardif, R., Michaelides, S. C., Cermak, J., Bott, A., Bendix, J., Müller, M. D., Pagowski, M., Hansen, B., Ellrod, G., and Others: Fog research: A review of past achievements and future perspectives, *Pure and Applied Geophysics*, 164, 1121–1159, 2007.
- Haefelin, M., Dupont, J. C., Boyouk, N., Baumgardner, D., Gomes, L., Roberts, G., and Elias, T.: A Comparative Study of Radiation Fog and Quasi-Fog Formation Processes During the ParisFog Field Experiment 2007, *Pure and Applied Geophysics*, 170, 2283–2303, <https://doi.org/10.1007/s00024-013-0672-z>, 2013.
- 685 Hammer, E., Gysel, M., Roberts, G. C., Elias, T., Hofer, J., Hoyle, C. R., Bukowiecki, N., Dupont, J.-C., Burnet, F., Baltensperger, U., and Weingartner, E.: Size-dependent particle activation properties in fog during the ParisFog 2012/13 field campaign, *Atmos. Chem. Phys*, 14, 10 517–10 533, <https://doi.org/10.5194/acp-14-10517-2014>, www.atmos-chem-phys.net/14/10517/2014/, 2014.
- Hill, A. A., Dobbie, S., and Yin, Y.: The impact of aerosols on non-precipitating marine stratocumulus. I: Model description and prediction of the indirect effect, *Quarterly Journal of the Royal Meteorological Society*, 134, 1143–1154, <https://doi.org/10.1002/qj.278>, <http://doi.wiley.com/10.1002/qj.278>, 2008.
- 690 IPCC: *Climate Change 2001: The Scientific Basis*, Cambridge University Press, 2001.
- Kiehl, J. T. and Trenberth, K. E.: Earth's Annual Global Mean Energy Budget, *Bulletin of the American Meteorological Society*, 78, 197–208, <http://journals.ametsoc.org/doi/abs/10.1175/1520-0477%281997%29078%3C0197%3AEAGMEB%3E2.0.CO%3B2>, 1997.

- 695 Lebo, Z. J., Morrison, H., and Seinfeld, J. H.: Are simulated aerosol-induced effects on deep convective clouds strongly dependent on saturation adjustment?, *Atmospheric Chemistry and Physics*, 12, 9941–9964, <https://doi.org/10.5194/acp-12-9941-2012>, 2012.
- Maalick, Z., Kühn, T., Korhonen, H., Kokkola, H., Laaksonen, A., and Romakkaniemi, S.: Effect of aerosol concentration and absorbing aerosol on the radiation fog life cycle, *Atmospheric Environment*, 133, 26–33, 2016.
- Malavelle, F. F., Haywood, J. M., Field, P. R., Hill, A. A., Abel, S. J., Lock, A. P., Shipway, B. J., and McBeath, K.: A method to represent subgrid-scale updraft velocity in kilometer-scale models: Implication for aerosol activation, *Journal of Geophysical Research: Atmospheres*, 119, 4149–4173, <https://doi.org/10.1002/2013JD021218>, <http://doi.wiley.com/10.1002/2013JD021218>, 2014.
- 700 Maronga, B. and Bosveld, F. C.: Key parameters for the life cycle of nocturnal radiation fog: a comprehensive large-eddy simulation study, *Quarterly Journal of the Royal Meteorological Society*, pp. 2463–2480, <https://doi.org/10.1002/qj.3100>, <http://doi.wiley.com/10.1002/qj.3100>, 2017.
- Mazoyer, M., Lac, C., Thouron, O., Bergot, T., Masson, V., and Musson-Genon, L.: Large eddy simulation of radiation fog: impact of dynamics on the fog life cycle, *Atmospheric Chemistry and Physics*, 17, 13 017–13 035, <https://doi.org/10.5194/acp-17-13017-2017>, <https://www.atmos-chem-phys.net/17/13017/2017/>, 2017.
- 705 Meskhidze, N., Nenes, A., Conant, W. C., and Seinfeld, J. H.: Evaluation of a new cloud droplet activation parameterization with in situ data from CRYSTAL-FACE and CSTRIFE, *Journal of Geophysical Research: Atmospheres*, 110, 2005.
- Miltenberger, A. K., Field, P. R., Hill, A. A., Rosenberg, P., Shipway, B. J., Wilkinson, J. M., Scovell, R., and Blyth, A. M.: Aerosol–cloud interactions in mixed-phase convective clouds – Part 1: Aerosol perturbations, *Atmospheric Chemistry and Physics*, 18, 3119–3145, <https://doi.org/10.5194/acp-18-3119-2018>, <https://www.atmos-chem-phys.net/18/3119/2018/>, 2018.
- 710 Morrison, H. and Gettelman, A.: A New Two-Moment Bulk Stratiform Cloud Microphysics Scheme in the Community Atmosphere Model, Version 3 (CAM3). Part I: Description and Numerical Tests, *Journal of Climate*, 21, 3642–3659, <https://doi.org/10.1175/2008JCLI2105.1>, <https://journals.ametsoc.org/doi/pdf/10.1175/2008JCLI2105.1>, 2008.
- 715 Nenes, A. and Seinfeld, J. H.: Parameterization of cloud droplet formation in global climate models, *Journal of Geophysical Research*, 108, <https://doi.org/10.1029/2002JD002911>, <http://doi.wiley.com/10.1029/2002JD002911>, 2003.
- Poku, C., Ross, A. N., Blyth, A. M., Hill, A. A., and Price, J. D.: How important are aerosol–fog interactions for the successful modelling of nocturnal radiation fog?, *Weather*, pp. 237–243, <https://doi.org/10.1002/wea.3503>, <https://rmets.onlinelibrary.wiley.com/doi/10.1002/wea.3503><https://rmets.onlinelibrary.wiley.com/doi/10.1002/wea.3503>, 2019.
- 720 Porson, A., Price, J., Lock, A., and Clark, P.: Radiation Fog. Part II: Large-Eddy Simulations in Very Stable Conditions, *Boundary-Layer Meteorology*, 139, 193–224, <https://doi.org/10.1007/s10546-010-9579-8>, <http://link.springer.com/10.1007/s10546-010-9579-8>, 2011.
- Price, J.: Radiation Fog. Part I: Observations of Stability and Drop Size Distributions, *Boundary-Layer Meteorology*, 139, 167–191, <https://doi.org/10.1007/s10546-010-9580-2>, 2011.
- 725 Price, J. D., Lane, S., Boutle, I. A., Smith, D. K. E., Bergot, T., Lac, C., Duconge, L., McGregor, J., Kerr-Munslow, A., Pickering, M., and Clark, R.: LANFEX: a field and modeling study to improve our understanding and forecasting of radiation fog, *Bulletin of the American Meteorological Society*, pp. 2061–2077, <https://doi.org/10.1175/BAMS-D-16-0299.1>, <http://journals.ametsoc.org/doi/10.1175/BAMS-D-16-0299.1>, 2018.
- Pruppacher, H. R. and Klett, J. D.: *Microphysics of Clouds and Precipitation*, vol. 18 of *Atmospheric and Oceanographic Sciences Library*, Springer, <https://doi.org/10.1007/978-0-306-48100-0>, <http://link.springer.com/10.1007/978-0-306-48100-0>, 2010.
- 730 Roach, W. T.: On some quasi-periodic oscillations observed during a field investigation of radiation fog, *Quarterly Journal of the Royal Meteorological Society*, 102, 355–359, <https://doi.org/10.1002/qj.49710243206>, <http://doi.wiley.com/10.1002/qj.49710243206>, 1976.

- Roach, W. T., Brown, R., Caughey, S. J., Garland, J. A., and Readings, C. J.: The physics of radiation fog: I - A field study, *Quarterly Journal of the Royal Meteorological Society*, 102, 313–333, 1976.
- Schwenkel, J. and Maronga, B.: Large-eddy simulation of radiation fog with comprehensive two-moment bulk microphysics: impact of different aerosol activation and condensation parameterizations, *Atmospheric Chemistry and Physics*, 19, 7165–7181, <https://doi.org/10.5194/acp-19-7165-2019>, <https://www.atmos-chem-phys.net/19/7165/2019/>, 2019.
- Schwenkel, J. and Maronga, B.: Towards a Better Representation of Fog Microphysics in Large-Eddy Simulations Based on an Embedded Lagrangian Cloud Model, *Atmosphere*, 11, 466, <https://doi.org/10.3390/atmos11050466>, <https://www.mdpi.com/2073-4433/11/5/466>, 2020.
- Seifert, A. and Heus, T.: Large-eddy simulation of organized precipitating trade wind cumulus clouds, *Atmospheric Chemistry and Physics*, 13, 5631–5645, <https://doi.org/10.5194/acp-13-5631-2013>, 2013.
- Shipway, B. J.: Revisiting Twomey’s approximation for peak supersaturation, *Atmospheric Chemistry and Physics*, 15, 3803–3814, 2015.
- Shipway, B. J. and Abel, S. J.: Analytical estimation of cloud droplet nucleation based on an underlying aerosol population, *Atmospheric Research*, 96, 344–355, <https://doi.org/10.1016/J.ATMOSRES.2009.10.005>, <https://www.sciencedirect.com/science/article/pii/S0169809509002798?via%3Dihub>, 2010.
- Shipway, B. J. and Hill, A. A.: Diagnosis of systematic differences between multiple parametrizations of warm rain microphysics using a kinematic framework, *Quarterly Journal of the Royal Meteorological Society*, 138, 2196–2211, <https://doi.org/10.1002/qj.1913>, <http://doi.wiley.com/10.1002/qj.1913>, 2012.
- Squires, P.: The Microstructure and Colloidal Stability of Warm Clouds: Part II-The Causes of the Variations in Microstructure, *Tellus*, 10, 262–271, <https://doi.org/10.3402/tellusa.v10i2.9228>, <https://www.tandfonline.com/doi/full/10.3402/tellusa.v10i2.9228>, 1958.
- Stolaki, S., Haefelin, M., Lac, C., Dupont, J.-C., Elias, T., and Masson, V.: Influence of aerosols on the life cycle of a radiation fog event. A numerical and observational study, *Atmospheric Research*, 151, 146–161, 2015.
- Taylor, G. I.: The formation of fog and mist, *Quarterly Journal of the Royal Meteorological Society*, 43, 241–268, <https://doi.org/10.1002/qj.49704318302>, <http://doi.wiley.com/10.1002/qj.49704318302>, 1917.
- Twomey, S.: The nuclei of natural cloud formation part II: The supersaturation in natural clouds and the variation of cloud droplet concentration, *Pure and Applied Geophysics*, 43, 243–249, 1959.
- Twomey, S.: Pollution and the planetary albedo, *Atmospheric Environment* (1967), 8, 1251–1256, 1974.
- Twomey, S.: The Influence of Pollution on the Shortwave Albedo of Clouds, *Journal of the Atmospheric Sciences*, 34, 1149–1152, 1977.
- Vie, B., Pinty, J. P., Berthet, S., and Leriche, M.: LIMA (v1.0): A quasi two-moment microphysical scheme driven by a multimodal population of cloud condensation and ice freezing nuclei, *Geoscientific Model Development*, 9, 567–586, <https://doi.org/10.5194/gmd-9-567-2016>, 2016.
- West, R. E. L., Stier, P., Jones, A., Johnson, C. E., Mann, G. W., Bellouin, N., Partridge, D. G., and Kipling, Z.: The importance of vertical velocity variability for estimates of the indirect aerosol effects, *Atmos. Chem. Phys*, 14, 6369–6393, <https://doi.org/10.5194/acp-14-6369-2014>, www.atmos-chem-phys.net/14/6369/2014/, 2014.
- Whitby, K. T.: The physical characteristics of sulfur aerosols, *Atmospheric Environment* (1967), 12, 135–159, 1978.
- WMO: International Meteorological Vocabulary, 1966.
- Young, G., Jones, H. M., Choularton, T. W., Crosier, J., Bower, K. N., Gallagher, M. W., Davies, R. S., Renfrew, I. A., Elvidge, A. D., Darbyshire, E., Marengo, F., Brown, P. R. A., Ricketts, H. M. A., Connolly, P. J., Lloyd, G., Williams, P. I., Allan, J. D., Taylor, J. W., Liu, D., and Flynn, M. J.: Observed microphysical changes in Arctic mixed-phase clouds when transitioning from sea ice to open ocean, *Atmos. Chem. Phys*, 16, 13 945–13 967, <https://doi.org/10.5194/acp-16-13945-2016>, www.atmos-chem-phys.net/16/13945/2016/, 2016.

770 Zhang, X., Musson-Genon, L., Dupont, E., Milliez, M., and Carissimo, B.: On the influence of a simple microphysics parametrization on radiation fog modelling: A case study during ParisFog, *Boundary-layer Meteorology*, 151, 293–315, 2014.